Titre: Title:	Inverse double diffusive natural convection problem in a porous medium
Auteur: Author:	Hui Jiang
Date:	2003
Type:	Mémoire ou thèse / Dissertation or Thesis
Référence: Citation:	Jiang, H. (2003). Inverse double diffusive natural convection problem in a porous medium [Master's thesis, École Polytechnique de Montréal]. PolyPublie. https://publications.polymtl.ca/7124/

In compliance with the
Canadian Privacy Legislation
some supporting forms
may have been removed from
this dissertation.

While these forms may be included
in the document page count,
their removal does not represent
any loss of content from the dissertation.

UNIVERSITÉ DE MONTRÉAL

INVERSE DOUBLE DIFFUSIVE NATURAL CONVECTION PROBLEM IN A POROUS MEDIUM

HUI JIANG
DÉPARTEMENT DE GÉNIE MÉCANIQUE
ÉCOLE POLYTECHNIQUE DE MONTRÉAL

MÉMOIRE PRÉSENTÉ EN VUE DE L'OBTENTION
DU DIPLÔME DE MAÎTRISE ÈS SCIENCES APPLIQUÉES
(GÉNIE MÉCANIQUE)
JUIN 2003

Your file Votre référence
ISBN: 0-612-86403-0
Our file Notre référence
ISBN: 0-612-86403-0

UNIVERSITÉ DE MONTRÉAL

ÉCOLE POLYTECHNIQUE DE MONTRÉAL

Ce mémoire intitulé:

INVERSE DOUBLE DIFFUSIVE NATURAL CONVECTION PROBLEM IN A POROUS MEDIUM

présenté par: JIANG Hui

en vue de l'obtention du diplôme de : Maîtrise ès sciences appliquées

a été dûment accepté par le jury d'examen constitué de :

M. VASSEUR Patrick, Ph.D., président

M. PRUD'HOMME Michel, Ph.D., membre et directeur de recherche

M. NGUYEN The Hung, Ph.D., member

Dedicated to my parents and my wife

ACKNOWLEDGEMENTS

First of all, I would like to express my greatest appreciation to Professor Michel Prud'homme, my master program supervisor, for his encouragement and guidance in all phase of my graduate studies in the department of mechanical engineering of École Polytechnique in the past two years. His patience, humor and wisdom have been permanently branded on my mind.

I would also like to acknowledge the invaluable help in many ways I received from Professor The Hung Nguyen. I am also very pleased to have the opportunity to work under his supervision and consultant in future study.

Thanks my wife and my parents for their love, support and help. I can't image that I would have enough courage and power to conquer various difficulties without their encouragement.

Finally I owe a debt of gratitude to École Polythechnique de Montréal for the wavier of the foreign student tuition fees and financial support during my studies at l'École Polythechnique.

RÉSUMÉ

L'objectif de ce mémoire est de résoudre le problème inverse de diffusion massique dans un milieu poreux bidimensionnel en présence de convection naturelle par la méthode du gradient conjugué et les équations adjointes. On établit le modèle mathématique de ce problème basé sur la loi de Darcy, l'approximation de Boussinesq, la loi de Fick et la conservation de masse et d'énergie. La démonstration des équations directes, des équations de sensibilité et des équations adjointes est fournie en détails. Le principe et le mécanisme de la méthode de l'optimisation sont présentés ensuite.

On utilise la méthode de volume contrôle pour faire la discrétisation pour toutes les équations différentielles avec la forme implicite et le schéma power-law. La méthode de Gauss—Seidel est aussi adoptée pour le calcul numérique par balayage de la ligne et colonne à chaque étape de temps. On utilise les coefficients de la relaxation pour empêcher la divergence des résultats. Toutes les solutions intégrales sont évoluées par la méthode de Simpson.

Le dernier chapitre présente les résultats numériques pour des cas différents. Les profils de concentration uniforme et non uniforme à la frontière active sont examinés pour les problèmes transitoires en supposant que les autres conditions frontières sont connues. D'excellents résultats peuvent être obtenus pour le problème inverse jusqu'à $Ra=10^4$ pour un profil uniforme. D'autre part, les solutions inverses ne sont pas très bien en accord avec les valeurs réelles pour le cas non uniforme. À partir des valeurs mesurées avec bruit, des solutions raisonnables sont obtenues selon le principe Alifanov si $\sigma \leq 0.05$.

ABSTRACT

The inverse double diffusive natural convection problem in a porous medium confined within a square enclosure is solved by conjugate gradient method and adjoint equations. The mathematical model is established based on the Darcy flow model, Boussinesq approximation, Fick's law and the conservation of momentum and energy. The derivation of the governing equations, the adjoint equations and the sensitivity equations is provided in detail. The principle and mechanism of the optimization method is introduced also.

All the partial differential equations are discretized using control volumes method with the power-law scheme and completely implicit form. Gauss—Seidel method is adopted to perform the iterative calculation by sweeping alternating line and column at each time step in the discrete system. The under relaxation coefficients are used to prevent the divergence of results. The integral solutions are numerically evaluated by Simpson's method.

Numerical results are presented for the unknown solute concentration profile on the active wall, assuming that the conditions for temperature and concentration on the remaining boundaries are given. Reasonably accurate solutions are obtained at least up to Ra = 10^4 for uniform profiles. On the other hand, the inverse solutions don't agree with the real values very well for non-uniform cases. In addition, noisy data solutions are effectively regularized according to the discrepancy principle of Alifanov.

CONDENSÉ EN FRANÇAIS

Le problème inverse devient de plus en plus important dans la société industrielle moderne. Présentement, beaucoup de domaines surtout de haute technologie rencontrent des problèmes inverses de transfert de chaleur tels que l'optimisation de design et la procédure de contrôle pour le chauffage, la détermination du coefficient de transfert de chaleur à la surface de missile ou d'avion etc.

Un problème inverse est considéré comme un problème mal posé mathématiquement. C'est–à–dire que la solution de ce problème n'existe pas, ou n'est pas unique, ou n'est pas une fonction continue des données. Durant les dernières années, les recherches des problèmes inverses en transfert de chaleur ont reçu un intérêt croissant à cause des développements des mathématiques appliquées et des technologies d'informatique.

La convection induite par les gradients de deux propriétés est connue comme convection de diffusion double. Les composants dans le système sont généralement la température et la concentration. Il y a beaucoup d'investigations des problèmes directs de convection naturelle avec double diffusion. Mais, les publications sur les problèmes inverses des transferts de chaleur et masse dans un milieu poreux sont rare. Quelques problèmes sont souvent rencontrés dans beaucoup des domaines par exemple océanographie, traitement de déchets, transport chimique dans le réacteur nucléaire, géographie, et d'autres domaines.

Il y a beaucoup de méthodes qui ont étés appliquées au problème inverse jusqu'à présent. Tikhonov a proposé la méthode de régularisation en 1963. Alifanov a développé cette approche directe et a présenté une méthode itérative de régularisation. Une autre méthode importante qui s'appelle temps futur est donnée dans le livre de Beck et al. En plus, d'autres methodes, par exemple l'approche probabilisable basée sur la théorie de Monte Carlo, qui joue un rôle important dans ce domaine. Dans mon étude, connue sous le nom de méthode du gradient conjugué est choisi pour résoudre le

problème inverse avec les équations adjointes. On a obtenu la solution parfaite si le profil de la concentration à la frontière active est uniforme.

Ce mémoire est divisé en six parties.

La première partie est une introduction expliquant les questions suivantes:

- Quel est le problème inverse?
- Quelle est la diffusion double?
- Quel est le milieu poreux?

Nous présentons ensuite l'histoire de développements du problème inverse de 1890 quand Stefan a obtenu la première solution exacte d'un problème inverse de conduction mono dimensionnelle à présent. Après nous définissons l'objectif de notre travail qui est la résolution du problème inverse de diffusion massique dans un milieu poreux bidimensionnel en présence de convection naturelle, en mesurant la concentration dans le système pour les différents cas.

Dans le chapitre I, nous définissons d'abord le problème que nous étudions en ce moment. La cavité rectangulaire rempli de milieu poreux est chauffée en bas et refroidi au sommet. Le mur gauche est le mur droit sont adiabatiques. Les débits de la concentration à travers le bas et le sommet sont zéro. La concentration au mur droit est aussi zéro. Quand t = 0, toutes les conditions initiales sont connues. Nous encastrons un senseur ou plusieurs dans le milieu poreux pour mesurer la concentration S_m. Notre objectif est de rechercher la concentration à la frontière active (le mur gauche) à partir de S_m. Nous établissons ensuite le modèle mathématique du problème direct basé sur la loi de Darcy, la loi de Fick et la loi de la conservation du moment et d'énergie. La démonstration des équations gouvernantes, i.e., l'équation continuité, l'équation du moment, l'équation d'énergie et l'équation de la diffusion massique, sont donné en détails. Pour simplifier ce modèle, nous utilisons la méthode de vorticité - fonction de

courant et en plus nous normalisons toutes les équations. Finalement, nous obtenons trois équations non dimensionnelles comme suit:

$$\nabla^2\psi = Ra_T\left(\frac{\partial T}{\partial x} + N\frac{\partial S}{\partial x}\right) = Ra_T\nabla_n \times \left(T\hat{g} + NS\hat{g}\right)$$

$$\frac{\partial T}{\partial t} + u\frac{\partial T}{\partial x} + v\frac{\partial T}{\partial y} = \frac{\partial^2 T}{\partial x^2} + \frac{\partial^2 T}{\partial y^2}$$

$$\varepsilon\frac{\partial S}{\partial t} + u\frac{\partial S}{\partial x} + v\frac{\partial S}{\partial y} = \frac{1}{Le}\left(\frac{\partial^2 S}{\partial x^2} + \frac{\partial^2 S}{\partial y^2}\right)$$

Où $u = \frac{\partial \psi}{\partial y}$, $v = -\frac{\partial \psi}{\partial x}$

On peut transformer un problème inverse en un problème d'optimisation. C'est – à – dire que la solution du problème inverse est obtenue par minimiser l'erreur *E*. Le deuxième chapitre présente la méthode d'optimisation qui est utilisée pour résoudre le problème inverse de double diffusion, i.e., la méthode du gradient conjugué. La direction de recherche et l'espace de marche sont déterminés par l'équation de sensibilité et l'équation adjointe. La démonstration mathématique de ces équations est fournie en détails dans ce chapitre. Nous présentons aussi la procédure d'optimisation par le gradient conjugué.

Le troisième chapitre décrit l'implémentation d'un code numérique. Nous faisons les discrétisations par la méthode de volume de contrôle avec la forme implicite et le schéma de loi de puissance proposée par Patankar pour toutes les équations. Dans les équations adjointes, un nouveau temps $\tau = t_f - t$ est défini à la place de temps physique *t*. Donc touts les paramètres adjoints sont calculés en temps final t_f. Par la voie de cette transformation, le coefficient de diffusion du problème adjoint devient positive, ceci peut améliorer la stabilité de la solution. Pour transférer l'information de la frontière à l'intérieur du système plus rapidement, nous faisons la un calcul itératif par la méthode de ligne-par-ligne. Et le calcul itératif entre deux lignes ou deux colonnes est exécuté

par la méthode de Gauss-Seidel. D'un autre côté, on peut choisir les coefficients de relaxation pour empêcher mieux converger. Dans la computation, quelques facteurs doivent être calculés par intégration. Ils sont évalués par la méthode de Simpson.

Le quatrième chapitre présente les solutions selon plusieurs profils de concentration prévues à la frontière active et d'autres conditions différentes. Nous comparons et discutons aussi touts les résultats obtenus pour analyser l'applicabilité de la méthode de gradient conjugué.

À la fin de ce mémoire, nous faisons les conclusions et les recommandations pour les travaux de recherche présents à partir des résultats et des discussions qui sont dans Chapitre IV. On peut prévoir précisément la concentration uniforme à la frontière active quand $0 < Ra \leq 10^4$, $0 < N \leq 10$ and $0 < Le \leq 5$. La solution du problème inverse n'est pas très sensible pour le facteur ε si il est moins que1.0. Pour plusieurs profils des concentrations prévues à la frontière active tels que la fonction linéaire, triangulaire, et de sinus etc., nous pouvons obtenir les solutions parfaites. Pour obtenir meilleurs résultats, les senseurs doivent être placés le plus prés de la frontière active si il est possible. Les conditions frontières peuvent influencer l'exactitude de la solution inverse. Les valeurs mesurées sont simulées par les données avec bruits. Nous obtenons les solutions acceptables jusqu'a $\sigma = 0.05$ selon la principe Alifanov. D'autre part, les solutions inverses ne sont pas très bien en accord avec les valeurs réelles pour les concentrations non uniformes prévues si le nombre de Rayleigh est grand.

TABLE OF CONTENTS

LIST OF FIGURES

LIST OF SYMBOLS

b	source term
C_a	active boundary
C_p	thermal capacity at constant pressure
D	mass diffusivity
E	object error function of optimization
f	friction factor or function
F	convection intensity or arbitrary parameter
g	gravitational acceleration or gradient fuction
H	height of the studied region
I	node position along x coordinate
J	node position along y coordinate
J_x, J_y	total flux along x direction and y direction
K	permeability
k	thermal conductivity, $W/(m \cdot K)$
L	length of studied region
Le	Lewis number
N	dimensionless ratio
n	normal direction
p	pressure
P	Searching direction
Pe	Peclet number
$\vec{r}$	position vector
Re	Reyleigh number
Re_T	thermal Darcy-Reyleigh number
S	concentration or source term
S_m	measured concentration
t	time

t_f	final time
T	temperature
u, v	scalar velocity
x, y	coordinates
Δx	mesh size along x
Δy	mesh size along y

Greek symbols

α	thermal diffusivity or optimal step size
β_T	thermal expansion coefficient
β_S	solute concentration expansion coefficient
μ	dynamic viscosity
ν	kinematic viscosity
σ	capacity ratio or error level
Ω	system surface
ψ	stream function
ω	vorticity
ε	normalized porosity or convergent criterion or arbitrary tiny real number
λ	step size
τ	time variable
Δ	increment
ρ	mass density
ϕ	porosity or arbitrary function
∇	gradient operator
$\nabla.$	divergence operator
$\nabla\times$	rotation operator
∇^2	Laplacian operator

Superscripts

$\bar{}$	adjoint variables
$\sim$	sensitivity variables
$*$	dimensionless variables or extremum value
k	iteration step

Subscripts

0	reference state
i	node series number in x coordinate
j	node series number in y coordinate
m	measured value
max	maximum value
min	minimum value
f	fluid
s	solid

Other symbols

$\langle \cdot \vert \cdot \rangle$	inner product
$\Vert \cdot \Vert$	norm
$\vert \cdot \vert$	modulus

INTRODUCTION

While seeing the title of this thesis, someone maybe asks the following questions:
What is the inverse problem?
What is double diffusion?
What is a porous medium?
Let's begin by answering these questions.

0.1 Inverse Heat Transfer Problems

In the last two decades, the research on inverse problems has undergone rapid development because of the needs of applications both in sciences and in industries. In various fields, such as signal and image processing, heat transfer, medical machines, bioelectric technique, the earth science, genetic algorithms and neural networks tutorial etc., the inverse problems are attracting the extensive attention.

Then, what is the inverse problem? J.B Keller [1] defined the inverse problem as: two problems are inverse to each other if the formulation of one problem involves the other one. Usually the simpler one or the one which was studied earlier is called direct problem, the other one is the inverse problem. Thus one might say inverse problems are concerned with determining causes for a desired or an observed effect [2]. O. M. Alifanov, the Russian proponent of inverse methods, probably said it best: solution of an inverse problem entails determining unknown causes based on observation of their effects. This is in contrast to the corresponding direct problem, whose solution involves finding effects based on a complete description of their causes [3].

For heat transfer problems, if the geometric shape of the system, boundary conditions, initial conditions, thermo-physical properties etc. are known, to determine the temperature distribution within a domain for example, is the direct problem; on the other hand, if the temperature of one point or some points within a system or on a part of the

bounding surface is obtained by measurement, to estimate the boundary conditions, inner heat source, or initial conditions etc. is the inverse problem.

One might classify the inverse problems according to their practical purpose such as inverse diagnostic problems, inverse control problems, and inverse design problems and so on. Of course, inverse problems may be classified arbitrarily. Another means of classification is by the type of information that is being sought in the solution procedure: backward or retrospective problem, coefficient inverse problem, and boundary inverse problem.

Inverse heat transfer problems might be encountered in many systems where the direct measurement of boundary conditions or the determination of thermo-physical properties of a system is impracticable. One typical example is related to the determination of the heat flux on the surface of a spacecraft or a missile. When the spacecraft reenters atmosphere, due to the aerodynamic effects, the temperature on the surface is so high that the thermo-physical properties cannot be measured directly. Some temperature sensors are embedded in the heat protective materials and the problem can be solved by inverse method. More practical applications include:

1. Heat measurement and thermal loading control;
2. One-dimensional heat flux sensors;
3. Parameter determination techniques;
4. Determination of contact thermal resistance;
5. Determination of frictional heat generation;
6. Optimization of design objectives;
7. Control of manufacturing process;
8. Applications in other domains.

More details can be found in [4].

Normally speaking, the inverse problem is much more difficult than the direct problem because:

1. The solutions of the inverse problems are unstable, i.e., very sensitive to the errors of measurements. A small error in input data can produce a physically unacceptable error in the solutions;
2. The response of the inner points to the changes of boundary conditions is attenuated and delayed.

Inverse problems are mathematically regarded as ill-posed problems, in the sense of Hadamard [5]. That means, they may have no solution, or if a solution exits, it might not be unique or not continuous with respect to the given data. Therefore they were considered to be unsolvable and of no practical or physical meaning. However the mathematicians and physicists have begun to change the attitude gradually since T. Carleman made the first attempt to solve an ill-posed problem [3]. The developments in applied mathematics and computer technology have made it possible to obtain *meaningful* solutions.

0.2 Double Diffusive Convection

Convection induced by the gradients of two properties with different molecular diffusivities is known as double diffusive convection. The components most commonly used in these systems have been temperature and concentration, and the corresponding case is called double diffusion flow or combined heat and mass transfer flow [6, 7].

In the 1800s, the studies of cirrus clouds almost led to the discovery of the mechanism of double diffusion. However a group of oceanographers made the discovery a full century later. The primary mechanism of double diffusion was formulated back in 1960 by Stern [8] as he considered *Perpetual Salt Fountain* experiment conceived by his colleagues (Stommel et al., 1956) a few years earlier for measuring deep ocean

pressures by lowering pipes from the surface [9]. And a fanciful idea soon developed into a theory of *Salt Fingers*. Stommel summarized the thought progression from salt fountain to salt fingers under the remarkable heading "Exciting Ten Minutes at the Blackboard". That means the central ideas of double diffusion research came to light in a short time [10].

In practice, double diffusive convection problems are frequently encountered in many domains, and not only in the ocean. For example, the disposal of waste materials, groundwater contamination, chemical transport in packed-bed reactors, grain-storage installations, food processing, soil research, fluidized-bed boiler and others [11]. The research on inverse double diffusive convection must extend the development of both the ill-posed problems and the double diffusion. Prud'homme and Jasmin have acquired the staggered production on this subject [12]. And it is likely to be of practical interest in non-pollution disposal of waste water by microbes. Double diffusive convection might occur in a porous medium or in a fluid (for example in ocean). My research focuses on the porous medium only.

0.3 Heat and Mass Transfer in Porous Medium

The problems of heat and mass transfer in porous media involve many engineering and science fields for example soil science, nuclear reactor cooling, mineral fuel mining, thermal insulation material, coal storage and combustion, desiccation of food and so on.

One hundred years ago, people started research on the porous medium. In 1856 a French physicist H. Darcy proposed the well-known Darcy's law during his investigation of ground water of Dijon city, France [13, 14]. In the 1950s the fluid flow in porous medium was developed to a science named "*Dynamics Fluids in Porous Media*". Nowadays the research of heat and mass transfer in porous medium has reached an unprecedented level, however the *Darcy model* is still the basic tool in this field.

The porous materials are multifarious, for example soil, ceramics, sand filter, bread, cooling bar of nuclear reactors etc. Initially, one attempts to describe a porous medium as "solid with holes". Obviously this definition is too rough. In fact porous medium consists of several substances with different phases (solid, liquid or gaseous). Any one phase is dispersed in the other phases. So porous medium sometimes is called "*dispersed material*". The pores in porous medium are interconnected, with at least several continuous paths, and by somehow specifying a better distribution (in either a regular or random manner) of holes and paths over the entire porous medium domain. Fluids can penetrate through this *effective pore space* from one side of the medium to another. So sometimes porous medium is also called "*permeable material*". Porous medium is not easy to define entirely and exactly. Bear, Zaslavsky and Irmay [14] defined porous medium in 1968 as follows:

- A portion of space occupied by heterogeneous or multiphase matter. The solid phase is called the solid matrix, and that space within the porous medium domain that is not part of the solid matrix is referred to as void space (or pore space).
- The solid phase should be distributed throughout the porous medium within the domain occupied by a porous medium; solid must be present inside each representative elementary volume.
- At least some of the pores comprising the void space should be interconnected.

Many experiences demonstrate that the irreversible transport processes may affect and disturb each other both in porous medium and in fluid. The reciprocities between wide sense "force" and wide sense "flux" is called *coupling effect* in *Irreversible Thermodynamics* [13]. J. Bear and Y. Bechmat [15] indicated that the thermal physical properties such as density, viscosity, surface tension and permeability etc. changing with temperature variation is the fundamental reason of coupling between heat transfer and mass transfer in multi-phases porous medium system.

Normally one "flux" may be driven by several "forces" and one "force" may drive several "fluxes". That is essence of coupling phenomenon. When the coupling phenomenon will happen? *Curie's law* gives us a key based on the tensor analysis since the "flux" and the "force" are tensors with different orders. In isotropic system, if the difference of tensor orders between the "fluxes" and "forces" are even (include zero), these "fluxes" and "forces" can be coupled. The detail may be found in [16].

0.4 Review of Literature

The earliest works on inverse problems are concerned with the determination of the historical climate and thermal conductivity of the earth's ground layer over a century ago. In 1890 Stefan obtained the first exact solution of the one-dimensional inverse heat conduction problem. Tyomkin and Burggraf got similar results in 1961 and 1964 for a series of other linear problems [3, 4]. Even though the first light of constructing solutions of inverse problems had already appeared in nineteenth century, the rapid growth happened only during the last twenty or thirty years. The enormous increase in computing power and the development of powerful algorithms made it possible to consider the various real-world problems and apply the techniques of inverse problems to ever more complicated systems.

For a long time scientists estimated parameters using optimization techniques. Some methods known long ago, for example the least squares criterion introduced by Legendre (1801) and Gauss (1809) were still used at present [17, 18, 19]. The 1960s and early 1970s was a golden age for the theory of inverse problems, lots of modern methods and algorithms appeared during this period. Wiggins, Franklin, Beck, Tikhonov, Burgrggraf and other pioneers made the great contributions to the theory of inverse problems. And the establishment of the complete mathematical theory system of inverse problems is chiefly based on the early works of these researchers. Tikhonov [20] proposed the well-known *regularization method* in 1963. His idea is considered as a milestone: *opening a fruitful direction in mathematical physics and computing*

mathematics, and considerably broadening the bounds of effective practical use of ill-posed problems in various fields of science and technology [3]. Tikhonov regularization is a direct method. The maximum entropy regularization [21], truncated total least squares, least squares with a quadratic constraint [22] and others also can be classified as *direct regularization methods.* Along this direction, Alifanov [3] proposed a so-called *iterative regularization.* Conjugate gradient method, the *v*-method and bidiagonalization with regularization are the best known iterative regularization methods. Another important regularizing technique is the so-called future time method introduced by Beck [23]. Murio developed the mollification technique to obtain smooth solutions [24, 25, 26].

Besides the regularizing technique, another famous genre is probabilistic approach. Purely probabilistic formulations of inverse theory appeared around 1970. Keilis-Borok and Yanovskaya founded Earth model by Monte Carlo theory in 1967 [27]. Bachus and Gilbert obtained the unknown function from discrete data in the years 1967-1970 [28]. Recently, the interest in Monte Carlo methods for the solution of inverse problems was increasing. Mosegaard and Tarantola proposed a gerneralization of Metropolis algorithm in 1995 [28]. More recently Monte Carlo analysis has been applied in real data inverse problems. One might believe, in the future, Monte Carlo method will still play an important role in the field of inverse problems.

The information preferred for our study is related to the inverse natural convection problems. Recently, many valuable contributions have been obtained on this topic based upon the various existing or new inverse approaches. The sequential function specification method [29] was used by Moutsoglou [30] to study inverse laminar natural convection in a fluid medium in a vertical channel. Park and Chung [31] and Park and Jung [32] solved the inverse natural convection problem using different approaches for an unknown time-dependent heat source inside a square cavity. Prud´homme and Nguyen [33] and Zabaras and Yang [34] used the conjugate gradient method with adjoint equations to study the inverse natural convection problem. But for inverse

double diffusive natural convection, few articles are published. More recently Prud'homme and Jasmin [12] adapted the conjugate gradient method to solve the inverse natural convection problem with mass diffusion in a porous medium. One may expect that the research on this subject will be led to further.

0.5 Objectives and Contents of the Thesis

Various inverse problems such as inverse heat conduction problems and inverse heat convection problems have been solved by the iterative conjugate gradient method with adjoint equations so far. How far one can go? Today we have not seen the end point. Extending the application of CGM in the inverse heat and mass transfer problems is the main purpose of my study. The objectives of this thesis can be summarized as follows:

1. Study the possibility of applying CGM in inverse double diffusive convection problems in porous medium;

2. Determine the range of Rayleigh number, Lewis number and other non-dimensional parameters, over which the stable inverse solutions can be obtained;

3. Investigate the cases of different concentration profiles on active boundary and different positions of measurement device;

4. Observe the influence of the random noise in input data upon the stability of solutions.

The contents of this thesis contain the following parts:

First of all, we introduce basic concept of inverse problem, double diffusion and heat and mass transfer in porous medium, review of literature and objective of this thesis.

In Chapter I, we establish the mathematical model for a double diffusive natural convection problem in a porous medium. The derivation of governing equations namely continuity equation, energy equation, mass diffusion equation and momentum equation is given in detail.

In Chapter II we apply the iterative conjugate gradient method in inverse heat and mass transfer problem in porous medium. The derivation of sensitivity equations and adjoint equations is given also.

In Chapter III, we discretize all partial differential equations for direct, sensitivity and adjoint problem with control volume method. The process and the algorithm of numerical computation are introduced.

In Chapter IV, we present and discuss various results with different cases.

Finally we draw conclusions based on the discussion of results for this study.

CHAPTER I
PROBLEM FORMULATION

1.1 Problem Description

Let's consider the two-dimensional rectangular porous cavity bounded by C sketched in Fig.1.1. The porous medium is homogeneous and isotropic. The bottom wall is heated and the top wall is cooled by uniform heat flux, and the horizontal walls are impermeable, i.e., at y=0 and y=H, $\frac{\partial T}{\partial y} = -1$ and $\frac{\partial S}{\partial x} = 0$. The temperature on vertical walls is uniform and constant, i.e., at $x = 0$ and $x = L$, $T = 0$. The last closure boundary condition is $S = 0$ at $x = L$. When $t = 0$, we suppose that the initial temperature and solute concentration fields are known. The sensors which are used to measure the concentration are embedded inside the porous medium. The symbol Ω denotes the surface of the 2-D system, while C_a stands for the active boundary (left wall). Our purpose is to determine the unknown solute concentration at x = 0 over the time interval $0 \le t \le t_f$, from the measured data S_m.

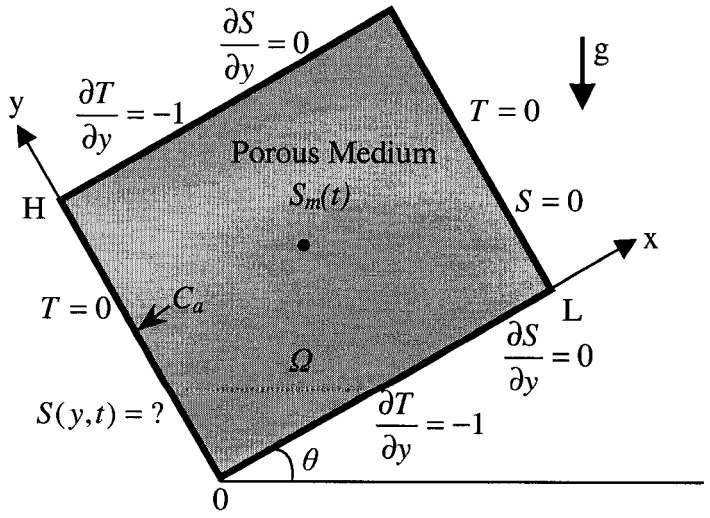

Figure 1.1 Geometry and Coordinates System

1.2 Assumptions

In order to simplify a double diffusive free convection problem in porous medium, Darcy flow model and Boussinesq approximation are usually adopted. The following assumptions [35] are necessary:

- The porous medium is homogeneous, isotropic, and in thermal equilibrium with the saturated fluid;
- The fluid is Newtonian (obeys Newton's viscous law), and obeys Boussinesq approximation, i.e., all physical properties of the fluid are considered as constant and independent of the temperature except the density that gives rise to the buoyancy force;
- All physical properties of the porous medium are considered as constant and independent of the temperature, time and space;
- The vorticity of the fluid at the boundaries are zero;
- The saturated fluid and porous matrix are incompressible;
- Viscous dissipation is negligible;
- No inner heat source.

1.3 Establishment of Mathematical Model

A physical phenomenon or process normally can be described by a series of theoretical or empirical formulas. The mathematical model of double diffusive free convection problem in porous medium is founded based on four governing equations. The derivation in detail is presented below.

1.3.1 Mass Conservation — Continuity Equation

The general two-dimensional continuity equation is:

$$\frac{\partial \rho}{\partial t}+\frac{\partial(\rho u)}{\partial x}+\frac{\partial(\rho v)}{\partial y}=\frac{\partial \rho}{\partial t}+\rho\frac{\partial u}{\partial x}+\rho\frac{\partial v}{\partial y}+u\frac{\partial \rho}{\partial x}+v\frac{\partial \rho}{\partial y}=0 \tag{1.1}$$

Since we have assumed that the fluid is incompressible, then:

$$\frac{D\rho}{Dt} = \frac{\partial \rho}{\partial t} + u\frac{\partial \rho}{\partial x} + v\frac{\partial \rho}{\partial y} = 0 \tag{1.2}$$

Substituting Eq.(1.2) into Eq.(1.1), we get the governing continuity equation:

$$\frac{\partial u}{\partial x} + \frac{\partial v}{\partial y} = 0 \tag{1.3}$$

1.3.2 Darcy Flow Model and Boussineq Approximation — Momentum Equation

About one hundred years ago, H. Darcy discovered that the area-average fluid velocity through a column of porous material is directly proportional to the pressure gradient established along the column based on numerous experimental observations and measurements. And subsequent experiments additionally proved that the area-average velocity of fluid is inversely proportional to the viscosity of the fluid. Darcy's law (one–dimension) can be represented mathematically as follow:

$$u = -\frac{K}{\mu}\frac{\partial p}{\partial x} \tag{1.4}$$

Doubtless, this is an empirical equation. Where K is a constant called *permeability*. It is a very important physical property of porous material. $K^{1/2}$ is a length scale representative of the effective pore diameter, so Reynolds number can be defined as:

$$\mathrm{Re} = \frac{uK^{1/2}}{\upsilon} \tag{1.5}$$

and the friction factor:

$$f = \frac{-\frac{dp}{dx}K^{1/2}}{\rho u^2} \tag{1.6}$$

Then we can get:

$$f \cdot \mathrm{Re} = \frac{-K\dfrac{dp}{dx}}{\mu u} \tag{1.7}$$

Substituting Eq. (1.4) into Eq. (1.7), we obtain:

$$f_{Darcy} = \frac{1}{\mathrm{Re}} \tag{1.8}$$

As long as $O(\mathrm{Re})<1$, the Eq. (1.4) and Eq.(1.8) are valid. These two equations are called *Darcy flow model.*

P.H. Forschheimer proposed a modification for the Darcy's law in 1901 [36] as follow:

$$-\frac{dp}{dx} = \frac{\mu}{K}u + b\rho u^2 \tag{1.9}$$

In where b is an empirical constant. If $O\left(\dfrac{uK^{1/2}}{\upsilon}\right) \geq 1$, we can't neglect the inertial effects and Darcy flow model should be replaced by Forschheimer-Darcy flow model.

In this thesis, we adopt Darcy's flow model to simply the problem, i.e., we assume that the pores are small enough so that:

$$O\left(\frac{uK^{1/2}}{\upsilon}\right) < 1 \tag{1.10}$$

If θ = 0, the Darcy's law in two-dimensional Cartesian coordinate (see Fig.1.1) becomes:

$$u = -\frac{K}{\mu}\frac{\partial p}{\partial x} \tag{1.11a}$$

$$v = -\frac{K}{\mu}\left(\frac{\partial p}{\partial y} + \rho g\right) \tag{1.11b}$$

A diffusive mass transfer process is inherently connected with heat transfer. In double diffusion, the density may vary with temperature as well as concentration. The density differential equation is as follow:

$$d\rho = \frac{\partial \rho}{\partial T} dT + \frac{\partial \rho}{\partial S} dS \tag{1.12}$$

The medium that saturates the porous matrix is treated as a Boussinesq incompressible fluid and its density can be expressed by following the linear equation:

$$\rho = \rho_0 [1 - \beta_T (T - T_0) - \beta_S (S - S_0)] \tag{1.13}$$

Here β_T is the thermal expansion coefficient and β_S is the concentration expansion coefficient. The subscript *0* denotes a reference state and:

$$\beta_T = -\frac{1}{\rho_0}\left(\frac{\partial \rho}{\partial T}\right)_{p,S} \tag{1.14}$$

$$\beta_S = -\frac{1}{\rho_0}\left(\frac{\partial \rho}{\partial S}\right)_{p,T} \tag{1.15}$$

Then Eq.(1.11b) becomes:

$$v = -\frac{K}{\mu}\left(\frac{\partial p}{\partial y} + \rho_0 g [1 - \beta_T (T - T_0) - \beta_S (S - S_0)]\right) \tag{1.16}$$

1.3.3 The First Law of Thermodynamics — Energy Equation

Obviously, heat and mass transfer in porous medium is different from that within a fluid. For the latter, there is no solid substance within the system; but for the former, we must consider the temperature variation of the porous matrix in the energy conservation equation.

If we neglect viscous dissipation and assume that there is no inner heat source and regard the porous structure as a homogenous medium, the energy equation in two-dimensional Cartesian coordinates can be written as:

$$[\phi\rho_f c_{Pf} + (1-\phi)\rho_s c_s]\frac{\partial T}{\partial t} + \rho_f c_{Pf}\left(u\frac{\partial T}{\partial x} + v\frac{\partial T}{\partial y}\right) = [\phi k_f + (1-\phi)k_s]\left(\frac{\partial^2 T}{\partial x^2} + \frac{\partial^2 T}{\partial y^2}\right) \quad (1.17)$$

where ϕ is a basic structure parameter of porous medium named *porosity*

The thermal conductivity of the porous medium k is defined as a combination of two conductivities namely:

$$k = \phi k_f + (1-\phi)k_s \quad (1.18)$$

In the same way， we define the capacity ratio as:

$$\sigma = \frac{\phi\rho_f c_{Pf} + (1-\phi)\rho_s c_s}{\rho_f c_{Pf}} \quad (1.19)$$

Then Eq.(1.17) becomes:

$$\rho_f c_f\left(\sigma\frac{\partial T}{\partial t} + u\frac{\partial T}{\partial x} + v\frac{\partial T}{\partial y}\right) = k\left(\frac{\partial^2 T}{\partial x^2} + \frac{\partial^2 T}{\partial y^2}\right) \quad (1.20)$$

The thermal diffusivity of the homogeneous porous medium is defined as:

$$\alpha = \frac{k}{\rho_f c_{Pf}} \quad (1.21)$$

From Eq.(1.20) and Eq.(1.21) we obtain the governing energy equation:

$$\sigma\frac{\partial T}{\partial t} + u\frac{\partial T}{\partial x} + v\frac{\partial T}{\partial y} = \alpha\left(\frac{\partial^2 T}{\partial x^2} + \frac{\partial^2 T}{\partial y^2}\right) \quad (1.22)$$

1.3.4 Fick's Law — Mass Diffusion Equation

Based on mass conservation and Fick's law, i.e., $\dot{m} = -D\frac{\partial S}{\partial n}$ (where $\dot{m}$ = is mass flux and D is mass diffusivity), we can easily write the mass diffusion equation as follow:

$$\phi\frac{\partial S}{\partial t}+u\frac{\partial S}{\partial x}+v\frac{\partial S}{\partial y}=D\left(\frac{\partial^2 S}{\partial x^2}+\frac{\partial^2 S}{\partial y^2}\right) \tag{1.23}$$

1.4 Simplification of Mathematical Model

The continuity equation, momentum equations, mass diffusion equation and energy equation govern the heat and mass transfer process in porous medium. These five equations with 5 unknown parameters (u, v, p, T, S) are closed by 8 coefficients namely ϕ, D, σ, α, K, μ, β_T, β_S. In this thesis, the pressure field is not the focus of the investigation. Then, is it possible to simplify the mathematical model to make it simpler and easier to handle? The answer is positive.

1.4.1 Vorticity-Stream Function Method

In momentum equations, the pressure gradient can't be neglected. To obtain a velocity field, we have to know the pressure field at first. The calculation of pressure is possible but it is much complicated also. If we can eliminate the pressure term, the problem will be easier. Fortunately, for two-dimensional problem, a so-called vorticity-stream function method [37] can help us to attain this goal.

We define vorticity as:

$$\omega=\frac{\partial v}{\partial x}-\frac{\partial u}{\partial y} \tag{1.24}$$

And stream function is defined as:

$$u=\frac{\partial \psi}{\partial y} \qquad v=-\frac{\partial \psi}{\partial x} \tag{1.25}$$

Because

$$\frac{\partial v}{\partial x}-\frac{\partial u}{\partial y}=-\left(\frac{\partial^2 \psi}{\partial x^2}+\frac{\partial^2 \psi}{\partial y^2}\right)=-\nabla^2\psi \tag{1.26}$$

Hence,

$$\omega = -\nabla^2\psi \tag{1.27}$$

From Eq. (1.11a) and Eq.(1.16) we can calculate the partial derivatives of scalar components of velocity:

$$\frac{\partial u}{\partial y} = -\frac{K}{\mu}\frac{\partial^2 p}{\partial y \partial x} \tag{1.28a}$$

$$\frac{\partial v}{\partial x} = -\frac{K}{\mu}\frac{\partial^2 p}{\partial x \partial y} - \frac{K}{\mu}\rho_0 g\left(\beta_T \frac{\partial T}{\partial x} + \beta_S \frac{\partial S}{\partial x}\right) \tag{1.28b}$$

Taking Eq. (1.28b) minus Eq. (1.28a), we get:

$$-\left(\frac{\partial v}{\partial x} - \frac{\partial u}{\partial y}\right) = \nabla^2\psi = -\omega = \frac{K}{\mu}\rho_0 g\left(\beta_T \frac{\partial T}{\partial x} + \beta_S \frac{\partial S}{\partial x}\right) \tag{1.29}$$

In this way, two momentum equations that include pressure term are simplified to a stream function equation.

1.4.2 Similarity Criterion and Non-Dimensional Equations

A physical process generally must be described by a considerable quantity of parameters. It brings us many difficulties. However the scientists found that some dimensionless groups that consist of several variables can describe certain phenomenon conveniently, these dimensionless groups are called *similarity criterion*. For example Reynolds number is usually used to estimate the status of the flow (laminar flow or turbulent flow) and Nusselt number can be used to estimate the intensity of the convection. Obviously, the adoption of the similarity theory and the similarity criterion simplifies the problems.

For the governing equations mentioned above, the dimensionless quantities might be defined as follows:

$$T^* = \frac{T - T_0}{\Delta T} \qquad u^* = \frac{Hu}{\alpha} \qquad v^* = \frac{Hv}{\alpha}$$

$$x^* = \frac{x}{H} \qquad y^* = \frac{y}{H} \qquad t^* = \frac{\alpha t}{\sigma H^2}$$

$$Ra_T = \frac{Kg\beta_T H\Delta T}{\alpha\upsilon} \qquad A = \frac{H}{L} \qquad \psi^* = \frac{\psi}{\alpha} \Rightarrow \nabla^2\psi^* = -\left(\frac{\partial v^*}{\partial x^*} - \frac{\partial u^*}{\partial y^*}\right)$$

$$Le = \frac{\alpha}{D} \qquad N = \frac{\beta_S \Delta S}{\beta_T \Delta T} \qquad S^* = \frac{S - S_0}{\Delta S}$$

where $\Delta T = \frac{q_{ref} H}{k}$, and Ra_T is the thermal Darcy-Rayleigh number based on the height.

So, $T = T^*\Delta T + T_0 \qquad u = \frac{\alpha}{H}u^* \qquad v = \frac{\alpha}{H}v^* \qquad S = S^*\Delta S + S_0$

$$x = Hx^* \qquad y = Hy^* \qquad t = \frac{\sigma H^2}{\alpha}t^*$$

(1.30)

Substituting expressions (1.30) into Eq. (1.29), we get:

$$-\left(\frac{\alpha}{H^2}\frac{\partial v^*}{\partial x^*} - \frac{\alpha}{H^2}\frac{\partial u^*}{\partial y^*}\right) = \frac{K}{\mu}\rho_0 g\left(\beta_T \frac{\Delta T}{H}\frac{\partial T^*}{\partial x^*} + \beta_S \frac{\Delta S}{H}\frac{\partial S^*}{\partial x^*}\right) \tag{1.31}$$

Hence

$$-\left(\frac{\partial v^*}{\partial x^*} - \frac{\partial u^*}{\partial y^*}\right) = \frac{Kg\beta_T \Delta T H}{\alpha\nu}\left(\frac{\partial T^*}{\partial x^*} + \frac{\beta_S \Delta S}{\beta_T \Delta T}\frac{\partial S^*}{\partial x^*}\right) \tag{1.32}$$

Namely

$$\nabla^2\psi^* = Ra_T\left(\frac{\partial T^*}{\partial x^*} + N\frac{\partial S^*}{\partial x^*}\right) \tag{1.33}$$

Substituting expressions (1.30) into Eq. (1.22), we get:

$$\sigma\frac{\Delta T\alpha}{\sigma H^2}\frac{\partial T^*}{\partial t^*}+\frac{\Delta T\alpha}{H^2}u^*\frac{\partial T^*}{\partial x^*}+\frac{\Delta T\alpha}{H^2}v^*\frac{\partial T^*}{\partial y^*}=\frac{\Delta T\alpha}{H^2}\left(\frac{\partial^2 T^*}{\partial x^{*2}}+\frac{\partial^2 T^*}{\partial y^{*2}}\right)$$

Namely

$$\frac{\partial T^*}{\partial t^*}+u^*\frac{\partial T^*}{\partial x^*}+v^*\frac{\partial T^*}{\partial y^*}=\frac{\partial^2 T^*}{\partial x^{*2}}+\frac{\partial^2 T^*}{\partial y^{*2}} \tag{1.34}$$

Similarly, substituting expressions (1.30) into Eq. (1.23), we get:

$$\frac{\phi}{\sigma}\frac{\Delta S\alpha}{H^2}\frac{\partial S^*}{\partial t^*}+\frac{\Delta S\alpha u^*}{H^2}\frac{\partial S^*}{\partial x^*}+\frac{\Delta S\alpha v^*}{H^2}\frac{\partial S^*}{\partial y^*}=\frac{\Delta SD}{H^2}\left(\frac{\partial^2 S^*}{\partial x^{*2}}+\frac{\partial^2 S^*}{\partial y^{*2}}\right) \tag{1.35}$$

We define normalized porosity of the porous medium ε as:

$$\varepsilon=\frac{\phi}{\sigma} \tag{1.36}$$

Then Eq.(1.36) becomes:

$$\varepsilon\frac{\partial S^*}{\partial t^*}+u^*\frac{\partial S^*}{\partial x^*}+v^*\frac{\partial S^*}{\partial y^*}=\frac{1}{Le}\left(\frac{\partial^2 S^*}{\partial x^{*2}}+\frac{\partial^2 S^*}{\partial y^{*2}}\right) \tag{1.37}$$

In the same way, non-dimensional stream function equations can be written as:

$$v^*=-\frac{\partial \psi^*}{\partial x^*},\qquad u^*=\frac{\partial \psi^*}{\partial y^*} \tag{1.38}$$

Omitting the superscript "*"from now, the non-dimensional Eq. (1.33), Eq. (1.34), Eq.(37) and Eq. (1.38) become:

$$\nabla^2\psi=Ra_T\left(\frac{\partial T}{\partial x}+N\frac{\partial S}{\partial x}\right)=Ra_T\nabla_n\times\left(T\,\hat{g}+NS\,\hat{g}\right) \tag{1.39}$$

$$\frac{\partial T}{\partial t}+u\frac{\partial T}{\partial x}+v\frac{\partial T}{\partial y}=\frac{\partial^2 T}{\partial x^2}+\frac{\partial^2 T}{\partial y^2} \tag{1.40}$$

$$\varepsilon\frac{\partial S}{\partial t}+u\frac{\partial S}{\partial x}+v\frac{\partial S}{\partial y}=\frac{1}{Le}\left(\frac{\partial^2 S}{\partial x^2}+\frac{\partial^2 S}{\partial y^2}\right) \tag{1.41}$$

$$u=\frac{\partial \psi}{\partial y} \tag{1.42}$$

$$v=-\frac{\partial \psi}{\partial x} \tag{1.43}$$

Eq.(1.39)~Eq.(1.41) construct the simplified model which include 3 unknown parameters (ψ, T, S) and 4 closure coefficients (Ra_T, N, ε, Le).

1.5 Direct Problem

For the direct problem, our objective is to determine the temperature field and concentration field based on established mathematical model by virtue of the given boundary conditions and initial conditions.

❖ Boundary Conditions

Generally there are three types of boundary conditions namely:

1. Dirichlet: $T\big|_w = Cons\tan t$

2. Neumann: $\left.\frac{\partial T}{\partial n}\right|_w = Cons\tan t$

3. Fourier: $\left(C_1 T + C_2\frac{\partial T}{\partial n}\right)\Big|_w = C_3$

According to the problem definition stated in *Section 1.1*, the boundary conditions can be written as follows:

At x =0 $\quad T = 0$

$S = f(y,t)$

$\psi = 0$

At x =L $\quad T = 0$

$S = 0$

$\psi = 0$

At $y = 0$ $\quad \dfrac{\partial T}{\partial y} = -1$

$\dfrac{\partial S}{\partial y} = 0$

$\psi = 0$

At y =H $\quad \dfrac{\partial T}{\partial y} = -1$

$\dfrac{\partial S}{\partial y} = 0$

$\psi = 0$

❖ **Initial Conditions**

We assume that: at t =0 $\quad T = 0,\ S = 0$ and $\psi = 0$

1.6 Inverse Problem

Suppose that the concentration $S_m(y, t)$ of one point or several points within the system is measured, initial conditions and all the boundary conditions except the concentration on active boundary (left wall) are given. The purpose of the inverse problem in this thesis is to seek the unknown concentration $S(0, y, t)$ during the time interval $0 \leq t \leq t_f$ under the following information:

At x =0 $\quad T = 0$

$\psi = 0$

At x =L $\quad T = 0$

$S = 0$

$\psi = 0$

At $y = 0$ $\quad \dfrac{\partial T}{\partial y} = -1$

$\dfrac{\partial S}{\partial y} = 0$

$\psi = 0$

At y =H $\quad \dfrac{\partial T}{\partial y} = -1$

$\dfrac{\partial S}{\partial y} = 0$

$\psi = 0$

At t =0 $\quad T = 0, S = 0$ and $\psi = 0$

And $S_m = S_m(y, t)$ is known

CHAPTER II
THE OPTIMIZATION METHOD FOR INVERSE PROBLEM

Since the inverse problems have an ill-posed character, the researchers always attempt to find a way to conquer this difficulty. Tikhonov, Alifanov, and others from the Russian school proposed to cast the inverse problem into an optimization problem with a regularized objective functional, and/or a self-regularizing algorithm of solution [3, 5]. Along this avenue, the iterative conjugate gradient method (CGM), one of the most stable algorithms, is widely used to solve the inverse problems today.

Then what is CGM? Let's review the mathematical background of the unconstrained optimization at first. And afterward, we will discuss the application of CGM in the inverse problem.

2.1 Unconstrained Optimization Method

Optimization is a branch of pure mathematics and might be defined as the science of determining the "best" solutions. Newton-like methods, steepest descend type methods, conjugate direction or conjugate gradient methods and restricted step methods can be classified as unconstrained optimization methods.

2.1.1 The Iterative Method

For an arbitrary function $f(x)$, $x \in R^n$, how to find the minimizing point? The iterative method is one of the most popular numerical methods. Its principle is as follow:

From an initial value $x^{(0)}$, calculate a series of $x^{(k)}$ (k=1, 2, 3, ...), the limit of the sequence $\{x^k\}$ is expected to give the extremum value x^*. As we know, the difference $x^{(k+1)} - x^{(k)}$ must be vector related to some gradient, in other words, $x^{(k+1)}$ might be described as:

$$x^{(k+1)} = x^{(k)} + \lambda_k P_k$$

where λ_k is a real number and is called *step size*, P_k is a vector and is called *searching direction*. The difference between the various iterative methods is how to determine the step size and the searching direction. But the basic rules are the same:

1) $f(x^{(0)}) \geq f(x^{(1)}) \geq \cdots \geq f\left(x^{(k)}\right) \geq \cdots$

2) The algorithm must be convergent.

2.1.2 The Gradient Method (Steepest Descent Method)

Let's consider an unconstrained minimizing problem:

$$\min f(x), \quad x \in E^n$$

Expand the function *f(x)* by Taylor series at the initial point $x^{(0)}$, we get:

$$f(x) = f\left(x^{(0)}\right) + \left(x - x^{(0)}\right)^T \nabla f\left(x^{(0)}\right) + o\left(\left\|x - x^{(0)}\right\|\right)$$

where $\nabla f\left(x^{(0)}\right)$ is the gradient of *f(x)* at the point $x^{(0)}$, and

$$\nabla f\left(x^{(0)}\right) = \begin{pmatrix} \dfrac{\partial f(x^{(0)})}{\partial x_1} \\ \dfrac{\partial f(x^{(0)})}{\partial x_2} \\ \vdots \\ \dfrac{\partial f(x^{(0)})}{\partial x_n} \end{pmatrix};$$

$\left(x - x^{(0)}\right)^T \nabla f\left(x^{(0)}\right)$ is the inner product of two vectors: $\left(x - x^{(0)}\right)^T$ and $\nabla f\left(x^{(0)}\right)$, where the superscript T stands for the matrix transpose; $\left\|x - x^{(0)}\right\|$ is the distance between x and $x^{(0)}$, when $\left\|x - x^{(0)}\right\| \to 0$, $\dfrac{o\left(\left\|x - x^{(0)}\right\|\right)}{\left\|x - x^{(0)}\right\|} \to 0$.

Let $x - x^{(0)} = \lambda P$, $\|P\| = 1$, $\lambda \geq 0$, if $x^{(0)}$ is not the minimizing point, the direction P satisfies $P^T \nabla f\left(x^{(0)}\right) < 0$ and if λ_0 is small enough, we must have:

$x^{(1)} = x^{(0)} + \lambda_0 P$ satisfies $f\left(x^{(1)}\right) < f\left(x^{(0)}\right)$.

Suppose λ is set, the value of $P^T\nabla f(x^{(0)})$ is smaller or the value of $-P^T\nabla f(x^{(0)})$ is larger, the function *f(x)* will descend faster. Obviously, when the angle between *P* and $\nabla f(x^{(0)})$ is equal to 180°, the value of $-P^T\nabla f(x^{(0)})$ will be the maximum:

$$\left(-P^T\nabla f(x^{(0)})\right)_{\max} = -\|P\|\|\nabla f(x^{(0)})\|\cos\pi = \|\nabla f(x^{(0)})\|$$

So along the opposite direction of the gradient of *f(x)* at $x^{(0)}$, *f(x)* descends fastest. Based on the discussion above, we might construct the iterative equation of the steepest descent method as follow:

$$x^{(k+1)} = x^{(k)} - \alpha_k \frac{\nabla f(x^{(k)})}{\|\nabla f(x^{(k)})\|} \quad \text{or}$$

$$x^{(k+1)} = x^{(k)} - \lambda_k \nabla f(x^{(k)})$$

Normally there are three classic ways to determine the step size λ_k:

- **Fixed Step Size Method**

  λ_k is a fixed value chosen by experience. This method is very simple. But it is very difficult to choose proper λ_k. If λ_k is too small, the convergence rate will be very slow; if it is too large, it may not satisfy $f(x^{(k+1)}) = f(x^{(k)} - \lambda_k\nabla f(x^{(k)})) < f(x^{(k)})$.

- **Optimization Step Size Method**

  λ_k satisfies $f(x^{(k+1)}) = f(x^{(k)} - \lambda_k\nabla f(x^{(k)})) = \min_{\lambda\geq 0} f(x^{(k)} - \lambda\nabla f(x^{(k)}))$.

  Generally speaking, this method is better than the fixed step size method. At the beginning, the convergence rate is fast. But when $f(x^{(k)})$ is close to the target value, the steepest descent method is no longer "steep".

- **PARTAN Method**

  In order to speed the convergence, Shah proposed PARTAN method. To calculate $x^{(1)}$, it is same as the optimization step size method. However, for the calculation of $x^{(k)}$ (k>1), it is different:

$$f(x^{(k)}) - \alpha_k\nabla f(x^{(k)}) = \min_{\lambda\geq 0} f(x^{(k)} - \lambda\nabla f(x^{(k)}))$$

$$y^{(k)} = x^{(k)} - \alpha_k \nabla f\left(x^{(k)}\right)$$

$$f\left(y^{(k)} - \lambda_k\left(y^{(k)} - x^{(k-1)}\right)\right) = \min_{\lambda \geq 0} f\left(y^{(k)} - \lambda\left(y^{(k)} - x^{(k-1)}\right)\right)$$

$$x^{(k+1)} = y^{(k)} - \lambda_k\left(y^{(k)} - x^{(k-1)}\right)$$

2.1.3 The Conjugate Gradient Method

The steepest descent method is simple, but its convergence rate and accuracy is poor for solving the complicated inverse problems. Instead, we choose the so-called conjugate gradient method which is based on the conjugate direction technique to regularize the inverse problems. Compared with the steepest descent method, it is more efficient and reliable, and the difference between these two methods is the determination of the searching direction. The step size is obtained by one dimensional search, which is also used in Partan method. In fact, for quadratic objective function, Partan method is equivalent with CGM.

The conjugate gradient method firstly applies to quadratic function only. And the derivation is also based on the quadratic function. Because it is too complicated, we won't discuss it here. The detail may be found in [38, 39].

There are several versions of conjugate gradient method, for example Daniel method, Hestenes-Stiefel method, Sorenson-Wolfe method, Polak-Ribiere method etc. [40]. Fletcher-Reeves method (1964), however, is considered as the representative of CGM because it is easy to remember and implement. For most versions of CGM, the searching direction can be expressed by the same form:

$$P^{(k+1)} = -g^{(k+1)} + \beta^{(k)} P^{(k)}$$

where $g^{(k+1)} = \nabla\left(f\left(x^{(k+1)}\right)\right)$, and $\beta^{(0)} = 0$

- Fletcher-Reeves method: $\beta^{(k)} = \dfrac{g^{(k+1)^T} g^{(k+1)}}{g^{(k)^T} g^{(k)}}$

- Polak-Ribiere method: $$\beta^{(k)} = \frac{\left(g^{(k+1)} - g^{(k)}\right)^T g^{(k+1)}}{g^{(k)^T} g^{(k)}}$$

- Sorenson-Wolfe method: $$\beta^{(k)} = \frac{-g^{(k+1)^T}\left(g^{(k+1)} - g^{(k)}\right)}{P^{(k)^T}\left(g^{(k+1)} - g^{(k)}\right)}$$

2.2 Application of Conjugate Gradient Method in Inverse Problem

An inverse problem such as stated in *Section 1.6* can be transformed to an unconstrained optimization problem. In other words, the inverse problem is solved by minimizing the error E to obtain unknown concentration $S = f(y, t)$, where the error is defined as:

$$E(f) = \frac{1}{2}\left\|S - S_m\right\|^2 \equiv \frac{1}{2}\int_0^{t_f}\sum_{i=1}^{n}\left(S - S_m\right)_i^2 \, dt \tag{2.1}$$

In the above, S and S_m stand respectively for the concentration predicted at the sensors from the approximation for f and the actual measurements, and i is number of sensors. If f is a function of time only, just a single sensor is needed to obtain a valid solution. If f also depends on y, a series of sensors will be required on a line parallel to the active boundary at all of the computational points.

Actually the objective values $f(y, t)$ are the minimizing points of error function $E(f)$. Then, theoretically speaking, the conjugate gradient method might be applied in this minimization problem. As we discussed in *Section 2.1*, $f(y, t)$ could be obtained by iterative computation according to $f^{(k+1)} = f^{(k)} + \alpha^k P^k$, where α^k is the step size and P^k is the conjugate search direction. Now new problems appear: how to determine the step size and the search direction? The search direction is related to the gradient of E, which can not be computed in the usual way without making assumptions about the shape of the function. The gradient of E, as well as the step size α, are obtained through solving the so-called adjoint and sensitivity equations.

2.2.1 The Sensitivity Problem

Firstly, let's introduce the concept of sensitivity. For an arbitrary parameter F which is function of a variable f, the sensitivity $\tilde{F}$ is the directional derivative of F at f in the direction Δf, i.e.,

$$D_{\Delta f}F = \tilde{F} = \lim_{\varepsilon \to 0} \frac{F(f + \varepsilon \Delta f) - F(f)}{\varepsilon} \tag{2.2}$$

According to the definition of the sensitivity stated above, we can get the temperature sensitivity $\tilde{T}$, concentration sensitivity $\tilde{S}$ and stream function sensitivity $\tilde{\psi}$ etc.

$$D_{\Delta f}T = \tilde{T} = \lim_{\varepsilon \to 0} \frac{T(f + \varepsilon \Delta f) - T(f)}{\varepsilon} \tag{2.3}$$

$$D_{\Delta f}S = \tilde{S} = \lim_{\varepsilon \to 0} \frac{(f + \varepsilon \Delta f) - f}{\varepsilon} \tag{2.4}$$

$$D_{\Delta f}\psi = \tilde{\psi} = \lim_{\varepsilon \to 0} \frac{\psi(f + \varepsilon \Delta f) - \psi(f)}{\varepsilon} \tag{2.5}$$

From the definition of the sensitivity namely Eq.(2.3) ~ Eq.(2.5), and the governing equations namely Eq.(1.39) ~ Eq.(1.41) it is straightforward to obtain the temperature, stream function and concentration sensitivity equations:

$$\nabla^2 \tilde{\psi} = Ra_T \nabla_n \times \left(\tilde{T}\, \hat{g} + N\tilde{S}\, \hat{g} \right) \tag{2.6}$$

$$\frac{\partial \tilde{T}}{\partial t} + \tilde{u}\frac{\partial T}{\partial x} + \tilde{v}\frac{\partial T}{\partial y} + u\frac{\partial \tilde{T}}{\partial x} + v\frac{\partial \tilde{T}}{\partial y} = \frac{\partial^2 \tilde{T}}{\partial x^2} + \frac{\partial^2 \tilde{T}}{\partial y^2} = \nabla^2 \tilde{T} \tag{2.7}$$

$$\varepsilon\frac{\partial \tilde{S}}{\partial t} + \tilde{u}\frac{\partial S}{\partial x} + \tilde{v}\frac{\partial S}{\partial y} + u\frac{\partial \tilde{S}}{\partial x} + v\frac{\partial \tilde{S}}{\partial y} = \frac{1}{Le}\left(\frac{\partial^2 \tilde{S}}{\partial x^2} + \frac{\partial^2 \tilde{S}}{\partial y^2} \right) = \frac{1}{Le}\nabla^2 \tilde{S} \tag{2.8}$$

Substituting continuity equation into Eq. (2.6) and Eq. (2.7) respectively we get:

$$\frac{\partial \tilde{T}}{\partial t} + \tilde{u}\frac{\partial T}{\partial x} + \tilde{v}\frac{\partial T}{\partial y} + u\frac{\partial \tilde{T}}{\partial x} + v\frac{\partial \tilde{T}}{\partial y} + \tilde{T}\left(\frac{\partial u}{\partial x} + \frac{\partial v}{\partial y} \right) + T\left(\frac{\partial \tilde{u}}{\partial x} + \frac{\partial \tilde{v}}{\partial y} \right) = \nabla^2 \tilde{T}$$

$$\varepsilon\frac{\partial\tilde{S}}{\partial t}+\tilde{u}\frac{\partial S}{\partial x}+\tilde{v}\frac{\partial S}{\partial y}+u\frac{\partial\tilde{S}}{\partial x}+v\frac{\partial\tilde{S}}{\partial y}+\tilde{S}\left(\frac{\partial u}{\partial x}+\frac{\partial v}{\partial y}\right)+S\left(\frac{\partial\tilde{u}}{\partial x}+\frac{\partial\tilde{v}}{\partial y}\right)=\frac{1}{Le}\nabla^2\tilde{S}$$

namely

$$\frac{\partial\tilde{T}}{\partial t}+\nabla\cdot\left(\tilde{\bar{u}}T+\bar{u}\tilde{T}\right)=\nabla^2\tilde{T} \tag{2.9}$$

$$\varepsilon\frac{\partial\tilde{S}}{\partial t}+\nabla\cdot\left(\tilde{\bar{u}}S+\bar{u}\tilde{S}\right)=\frac{1}{Le}\nabla^2\tilde{S} \tag{2.10}$$

The boundary condition for the sensitivity remains identical with that of the direct problem except on the active boundary C_a.

$$\tilde{\psi}\big|_C=0$$

$$\frac{\partial\tilde{T}}{\partial y}\Big|_{y=0,H}=0$$

$$\tilde{T}\big|_{x=0,L}=0$$

$$\frac{\partial\tilde{S}}{\partial y}\Big|_{y=0,L}=0$$

$$\tilde{S}\big|_{x=L}=0$$

$$\tilde{S}\big|_{x=0}=\Delta f$$

2.2.2 The Adjoint Problem

Starting from Eq.(2.1), the directional derivative of E in the direction Δf is defined as:

$$D_{\Delta f}E(f)=\left\langle\nabla E\middle|\Delta f\right\rangle=\left\langle S-S_m\middle|\tilde{S}\right\rangle \tag{2.11}$$

Where the symbol $\langle\cdot|\cdot\rangle$ stands for inner product.

The right-hand side of Eq.(2.11) may be expressed as an integral over surface and time using *Dirac's* delta function:

$$D_{\Delta f}E(f)=\int_0^{t_f}\sum_{i=1}^{n}\left(S-S_m\right)_i\,\tilde{S}_i\,dt=\int_0^{t_f}\int_{\Omega}\left(S-S_m\right)\tilde{S}\sum_{i=1}^{n}\delta(\vec{r}-\vec{r}_i)\,dAdt \tag{2.12}$$

In order to determine ∇E, we adopt *Lagrange Multiplier Method* and regard the so-called adjoint temperature $\overline{T}$, adjoint stream function $\overline{\psi}$ and adjoint concentration $\overline{S}$ as *Lagrange multipliers* for the sensitivity equations Eq.(2.9), Eq.(2.6) and Eq.(2.10). It is possible to rewrite Eq.(2.12) as:

$$\begin{aligned}
D_{\Delta f}E(f)=&\int_0^{t_f}\int_{\Omega}\left(S-S_m\right)\tilde{S}\sum_{i=1}^{n}\delta(\vec{r}-\vec{r}_i)\,dAdt\\
&+\int_0^{t_f}\int_{\Omega}\overline{\psi}\left\{\nabla^2\tilde{\psi}-\mathrm{R}a_T\nabla_n\times(\tilde{T}+N\tilde{S})\hat{\mathbf{g}}\right\}dAdt\\
&+\int_0^{t_f}\int_{\Omega}\overline{T}\left\{\frac{\partial\tilde{T}}{\partial t}+\nabla\cdot\left(\bar{u}\tilde{T}+\tilde{\bar{u}}T\right)-\nabla^2\tilde{T}\right\}dAdt\\
&+\int_0^{t_f}\int_{\Omega}\overline{S}\left\{\varepsilon\frac{\partial\tilde{S}}{\partial t}+\nabla\cdot\left(\bar{u}\tilde{S}+\tilde{\bar{u}}S\right)-\frac{\nabla^2\tilde{S}}{Le}\right\}dAdt
\end{aligned} \tag{2.13}$$

The general *Green's identity* is as follow:

$$\int_D\left(u\nabla^2v-v\nabla^2u\right)d(x,y)=\int_C\left(u\frac{\partial v}{\partial n}-v\frac{\partial u}{\partial n}\right)ds$$

According to Green's identity, the second term of the right side of Eq.(2.13) can be transformed as follow:

$$\begin{aligned}
&\int_0^{t_f}\int_{\Omega}\overline{\psi}\left\{\nabla^2\tilde{\psi}-Ra_T\nabla_n\times\left(\tilde{T}\,\hat{g}+N\tilde{S}\,\hat{g}\right)\right\}dAdt\\
&=\int_0^{t_f}\int_{\Omega}\left\{\left(\overline{\psi}\nabla^2\tilde{\psi}-\tilde{\psi}\nabla^2\overline{\psi}\right)+\tilde{\psi}\nabla^2\overline{\psi}-Ra_T\overline{\psi}\nabla_n\times\left(\tilde{T}\,\hat{g}+N\tilde{S}\,\hat{g}\right)\right\}dAdt\\
&=\int_0^{t_f}\int_C\left(\overline{\psi}\frac{\partial\tilde{\psi}}{\partial n}-\tilde{\psi}\frac{\partial\overline{\psi}}{\partial n}\right)dldt+\int_0^{t_f}\int_{\Omega}\left\{\tilde{\psi}\nabla^2\overline{\psi}-Ra_T\overline{\psi}\nabla_n\times\left(\tilde{T}\,\hat{g}+N\tilde{S}\,\hat{g}\right)\right\}dAdt
\end{aligned} \tag{2.14}$$

In the same way, the third term of the right side of Eq. (2.13) can be transformed as follow:

$$\begin{aligned}
&\int_0^{t_f}\int_\Omega \overline{T}\left\{\frac{\partial \tilde{T}}{\partial t}+\nabla\cdot\left(\tilde{\vec{u}}T+\vec{u}\tilde{T}\right)-\nabla^2\tilde{T}\right\}dAdt \\
&=\int_0^{t_f}\int_\Omega\left\{\left[\overline{T}\frac{\partial \tilde{T}}{\partial t}+\overline{T}\nabla\cdot\left(\tilde{\vec{u}}T+\vec{u}\tilde{T}\right)-\tilde{T}\nabla^2\overline{T}\right]+\left(\tilde{T}\nabla^2\overline{T}-\overline{T}\nabla^2\tilde{T}\right)\right\}dAdt \qquad (2.15)\\
&=\int_0^{t_f}\int_C\left(\tilde{T}\frac{\partial \overline{T}}{\partial n}-\overline{T}\frac{\partial \tilde{T}}{\partial n}\right)dldt+\int_0^{t_f}\int_\Omega\left\{\overline{T}\frac{\partial \tilde{T}}{\partial t}+\overline{T}\nabla\cdot\left(\tilde{\vec{u}}T+\vec{u}\tilde{T}\right)-\tilde{T}\nabla^2\overline{T}\right\}dAdt
\end{aligned}$$

Because

$$\begin{aligned}
\overline{T}\nabla\cdot\left(\tilde{\vec{u}}T+\vec{u}\tilde{T}\right)&=\nabla\cdot\left(\vec{u}\tilde{T}\overline{T}+\tilde{\vec{u}}T\overline{T}\right)-\tilde{T}(\vec{u}\cdot\nabla)\overline{T}-T\left(\tilde{\vec{u}}\cdot\nabla\right)\overline{T}\\
&=\nabla\cdot\left(\vec{u}\tilde{T}\overline{T}+\tilde{\vec{u}}T\overline{T}\right)-\tilde{T}\nabla\cdot\left(\vec{u}\overline{T}\right)+\overline{T}\nabla\cdot\vec{u}-T\left(\tilde{\vec{u}}\cdot\nabla\right)\overline{T}\\
&=\nabla\cdot\left(\vec{u}\tilde{T}\overline{T}+\tilde{\vec{u}}T\overline{T}\right)-\tilde{T}\nabla\cdot\left(\vec{u}\overline{T}\right)-T\left(\tilde{\vec{u}}\cdot\nabla\right)\overline{T}
\end{aligned}$$

So Eq. (2.15) becomes

$$\begin{aligned}
\int_0^{t_f}\int_\Omega \overline{T}\left\{\frac{\partial \tilde{T}}{\partial t}+\nabla\cdot\left(\tilde{\vec{u}}T+\vec{u}\tilde{T}\right)-\nabla^2\tilde{T}\right\}dAdt&=\int_0^{t_f}\int_C\left(\tilde{T}\frac{\partial \overline{T}}{\partial n}-\overline{T}\frac{\partial \tilde{T}}{\partial n}\right)dldt+\int_0^{t_f}\int_\Omega\nabla\cdot\left(\vec{u}\tilde{T}\overline{T}+\tilde{\vec{u}}T\overline{T}\right)dAdt\\
&\quad+\int_0^{t_f}\int_\Omega\left\{\overline{T}\frac{\partial \tilde{T}}{\partial t}-\tilde{T}\nabla\cdot\left(\vec{u}\overline{T}+\nabla\overline{T}\right)-T\left(\tilde{\vec{u}}\cdot\nabla\right)\overline{T}\right\}dAdt
\end{aligned} \qquad (2.16)$$

By virtue of divergence theory and the impermeability boundary condition namely $\vec{u}_n\big|_C=0$, we may get:

$$\int_0^{t_f}\int_\Omega\nabla\cdot\left(\vec{u}\tilde{T}\overline{T}+\tilde{\vec{u}}T\overline{T}\right)dAdt=\int_0^{t_f}\int_C\overline{T}\left(\tilde{T}\vec{u}_n+T\tilde{u}_n\right)dldt=0 \qquad (2.17)$$

Then Eq.(2.16) becomes

$$\int_0^{t_f}\int_\Omega \overline{T}\left\{\frac{\partial \tilde{T}}{\partial t}+\nabla\cdot\left(\bar{\tilde{u}}T+\bar{u}\tilde{T}\right)-\nabla^2\tilde{T}\right\}dAdt=\int_0^{t_f}\int_C\left(\tilde{T}\frac{\partial \overline{T}}{\partial n}-\overline{T}\frac{\partial \tilde{T}}{\partial n}\right)dldt$$
$$+\int_0^{t_f}\int_\Omega\left\{\overline{T}\frac{\partial \tilde{T}}{\partial t}-\tilde{T}\nabla\cdot\left(\bar{u}\overline{T}+\nabla\overline{T}\right)-T\left(\bar{\tilde{u}}\cdot\nabla\right)\overline{T}\right\}d\Omega dt \tag{2.18}$$

Similarly, the fourth term of the right side of Eq. (2.13) can be transformed as follow:

$$\int_0^{t_f}\int_\Omega \overline{S}\left\{\varepsilon\frac{\partial \tilde{S}}{\partial t}+\nabla\cdot\left(\bar{\tilde{u}}S+\bar{u}\tilde{S}\right)-\frac{1}{Le}\nabla^2\tilde{S}\right\}dAdt$$
$$=\frac{1}{Le}\int_0^{t_f}\int_C\left(\tilde{S}\frac{\partial \overline{S}}{\partial n}-\overline{S}\frac{\partial \tilde{S}}{\partial n}\right)dldt+\int_0^{t_f}\int_\Omega\left\{\varepsilon\overline{S}\frac{\partial \tilde{S}}{\partial t}-\tilde{S}\nabla\cdot\left(\bar{u}\overline{S}+\frac{1}{Le}\nabla\overline{S}\right)-S\left(\bar{\tilde{u}}\cdot\nabla\right)\overline{S}\right\}dAdt \tag{2.19}$$

The first terms of the right side of Eq. (2.14) and Eq. (2.18) are equal to zero namely:

$$\int_0^{t_f}\int_C\left(\overline{\psi}\frac{\partial \tilde{\psi}}{\partial n}-\tilde{\psi}\frac{\partial \overline{\psi}}{\partial n}\right)dldt=0 \tag{2.20}$$

$$\int_0^{t_f}\int_C\left(\tilde{T}\frac{\partial \overline{T}}{\partial n}-\overline{T}\frac{\partial \tilde{T}}{\partial n}\right)dldt=0 \tag{2.21}$$

and the first terms of the right side of Eq. (2.19)

$$\frac{1}{Le}\int_0^{t_f}\int_C\left(\tilde{S}\frac{\partial \overline{S}}{\partial n}-\overline{S}\frac{\partial \tilde{S}}{\partial n}\right)dldt=\frac{1}{Le}\int_0^{t_f}\int_{C_a}\left(\tilde{S}\frac{\partial \overline{S}}{\partial n}\right)dldt=\frac{1}{Le}\int_0^{t_f}\int_{C_a}\left(\frac{\partial \overline{S}}{\partial n}\Delta f\right)dldt \tag{2.22}$$

If we require such boundary conditions for $\overline{\psi}$, $\overline{T}$ and $\overline{S}$ as:

$\overline{\psi}\big|_C=0$;

$\overline{T}$ =0 where T is known or/and $\frac{\partial \overline{T}}{\partial n}=0$ where $\frac{\partial T}{\partial n}$ is known;

$\overline{S}$ =0 where S is known or on the active boundary or/and $\frac{\partial \overline{S}}{\partial n}=0$ where $\frac{\partial S}{\partial n}$ is known.

From the definition of stream function, we also have

$$
\begin{aligned}
T\left(\tilde{\vec{u}}\cdot\nabla\right)\overline{T} &= T\tilde{\psi}_y\overline{T}_x - T\tilde{\psi}_x\overline{T}_y = \left(T\tilde{\psi}\right)_y\overline{T}_x - \left(T\tilde{\psi}\right)_x\overline{T}_y - \overline{\psi}T_y\overline{T}_x + \tilde{\psi}T_x\overline{T}_y \\
&= \left(T\tilde{\psi}\overline{T}_x\right)_y - \left(T\tilde{\psi}\overline{T}_y\right)_x + \tilde{\psi}\left(T_x\overline{T}_y - \overline{T}_xT_y\right) \\
&= \tilde{\psi}\frac{\partial\left(T,\overline{T}\right)}{\partial\left(x,y\right)} - \nabla_n\times\left(T\tilde{\psi}\nabla\overline{T}\right)
\end{aligned}
\tag{2.23}
$$

Thus, according to *Stoke's* theorem,

$$
\begin{aligned}
\int_0^{t_f}\int_\Omega T\left(\tilde{\vec{u}}\cdot\nabla\right)\overline{T}\,dA\,dt &= \int_0^{t_f}\int_\Omega \tilde{\psi}\frac{\partial\left(T,\overline{T}\right)}{\partial\left(x,y\right)}dA\,dt - \int_0^{t_f}\int_\Omega \nabla_n\times\left(T\tilde{\psi}\nabla\overline{T}\right)dA\,dt \\
&= \int_0^{t_f}\int_\Omega \tilde{\psi}\frac{\partial\left(T,\overline{T}\right)}{\partial\left(x,y\right)}dA\,dt - \int_0^{t_f}\int_C T\tilde{\psi}\left(\nabla\overline{T}\right)_n dl\,dt
\end{aligned}
\tag{2.24}
$$

Since $\tilde{\psi}\big|_C = 0$, then

$$
\int_0^{t_f}\int_C T\tilde{\psi}\left(\nabla\overline{T}\right)_n dl\,dt = 0
$$

So

$$
\int_0^{t_f}\int_\Omega T\left(\tilde{\vec{u}}\cdot\nabla\right)\overline{T}\,dA\,dt = \int_0^{t_f}\int_\Omega \tilde{\psi}\frac{\partial\left(T,\overline{T}\right)}{\partial\left(x,y\right)}dA\,dt \tag{2.25}
$$

Similarly, we can obtain:

$$
\int_0^{t_f}\int_\Omega S\left(\tilde{\vec{u}}\cdot\nabla\right)\overline{S}\,dA\,dt = \int_0^{t_f}\int_\Omega \tilde{\psi}\frac{\partial\left(S,\overline{S}\right)}{\partial\left(x,y\right)}dA\,dt \tag{2.26}
$$

The conclusion of the discussion above, based on Eq.(2.14), Eq.(2.18), Eq.(2.19), Eqs. (2.20)~(2.22), Eq. (2.25) and Eq. (2.26), is therefore that Eq. (2.13) becomes

$$
\begin{aligned}
D_{\Delta f}E = & \int_0^{t_f}\iint_{\Omega}(S-S_m)\tilde{S}\sum_{i=1}^{n}\delta(\vec{r}-\vec{r}_i)\,dAdt + \frac{1}{\mathrm{Le}}\int_0^{t_f}\int_{C_a}\frac{\partial\bar{S}}{\partial n}\Delta f dl dt \\
& + \int_0^{t_f}\iint_{\Omega}\left\{\bar{\psi}\left(\nabla^2\bar{\psi} - \frac{\partial(T,\bar{T})}{\partial(x,y)} - \frac{\partial(S,\bar{S})}{\partial(x,y)}\right) - Ra_T\bar{\psi}\nabla_n\times\left(\tilde{T}\,\hat{g} + N\tilde{S}\,\hat{g}\right)\right\}dAdt \\
& + \int_0^{t_f}\iint_{\Omega}\left\{\bar{T}\frac{\partial\tilde{T}}{\partial t} - \tilde{T}\nabla\cdot\left(\vec{u}\bar{T} + \nabla\bar{T}\right)\right\}dAdt \\
& + \int_0^{t_f}\iint_{\Omega}\left\{\varepsilon\bar{S}\frac{\partial\tilde{S}}{\partial t} - \tilde{S}\nabla\cdot\left(\vec{u}\bar{S} + \frac{1}{Le}\nabla\bar{S}\right)\right\}dAdt
\end{aligned}
\tag{2.27}
$$

Since gravity is a constant vector, we have

$$
\bar{\psi}\nabla_n\times\left(\tilde{T}\,\hat{g} + N\tilde{S}\,\hat{g}\right) = \nabla_n\times\left(\bar{\psi}\tilde{T}\,\hat{g} + N\bar{\psi}\tilde{S}\,\hat{g}\right) - \left(\tilde{T} + N\tilde{S}\right)\nabla_n\times\left(\bar{\psi}\,\hat{g}\right)
$$

So by stoke"s theorem

$$
\int_0^{t_f}\iint_{\Omega}\left\{\bar{\psi}\nabla_n\times\left(\tilde{T}\,\hat{g} + N\tilde{S}\,\hat{g}\right)\right\}dAdt \overset{Stoke'sTheorem}{=} \int_0^{t_f}\int_C\bar{\psi}\left(\tilde{T} + N\tilde{S}\right)\hat{g}\,dldt - \int_0^{t_f}\iint_{\Omega}\left(\tilde{T} + N\tilde{S}\right)\nabla_n\times\left(\bar{\psi}\,\hat{g}\right)dAdt
$$

Since $\bar{\psi}\big|_C = 0$, then

$$
\int_0^{t_f}\int_C\bar{\psi}\left(\tilde{T} + N\tilde{S}\right)\hat{g}\,dldt = 0
$$

thus

$$
\iint_{t,\Omega}\left\{\bar{\psi}\nabla_n\times\left(\tilde{T}\,\hat{g} + N\tilde{S}\,\hat{g}\right)\right\}d\Omega dt = -\iint_{t,\Omega}\left(\tilde{T} + N\tilde{S}\right)\nabla_n\times\left(\bar{\psi}\,\hat{g}\right)d\Omega dt \tag{2.28}
$$

Therefore, Eq.(2.27) becomes

$$
\begin{aligned}
D_{\Delta f}E = &\int_0^{t_f}\int_{\Omega}(S-S_m)\tilde{S}\sum_{i=1}^{n}\delta(\vec{r}-\vec{r}_i)\,dAdt+\frac{1}{\mathrm{Le}}\int_0^{t_f}\int_{C_a}\frac{\partial\bar{S}}{\partial n}\Delta f dl dt\\
&+\int_0^{t_f}\int_{\Omega}\left\{\tilde{\psi}\left(\nabla^2\bar{\psi}-\frac{\partial(T,\bar{T})}{\partial(x,y)}-\frac{\partial(S,\bar{S})}{\partial(x,y)}\right)\right\}dAdt\\
&+\int_0^{t_f}\int_{\Omega}\left\{\bar{T}\frac{\partial\tilde{T}}{\partial t}-\tilde{T}\nabla\cdot\left(\vec{u}\bar{T}+\nabla\bar{T}\right)+Ra_T\tilde{T}\nabla_n\times\left(\bar{\psi}\,\hat{g}\right)\right\}dAdt\\
&+\int_0^{t_f}\int_{\Omega}\left\{\varepsilon\bar{S}\frac{\partial\tilde{S}}{\partial t}-\tilde{S}\nabla\cdot\left(\vec{u}\bar{S}+\frac{1}{Le}\nabla\bar{S}\right)+Ra_TN\tilde{S}\nabla_n\times\left(\bar{\psi}\,\hat{g}\right)\right\}dAdt
\end{aligned}
\tag{2.29}
$$

If we assume that the adjoint variables all vanish at $t = t_f$, namely

$$\bar{T}\Big|_{t=t_f}=0$$

$$\bar{S}\Big|_{t=t_f}=0$$

we may write

$$\int_0^{t_f}\int_{\Omega}\bar{T}\frac{\partial\tilde{T}}{\partial t}dAdt=\int_0^{t_f}\int_{\Omega}\frac{\partial(\bar{T}\tilde{T})}{\partial t}dAdt-\int_0^{t_f}\int_{\Omega}\tilde{T}\frac{\partial\bar{T}}{\partial t}dAdt=-\int_0^{t_f}\int_{\Omega}\tilde{T}\frac{\partial\bar{T}}{\partial t}dAdt \tag{2.30}$$

$$\int_0^{t_f}\int_{\Omega}\bar{S}\frac{\partial\tilde{S}}{\partial t}dAdt=\int_0^{t_f}\int_{\Omega}\frac{\partial(\bar{S}\tilde{S})}{\partial t}dAdt-\int_0^{t_f}\int_{\Omega}\tilde{S}\frac{\partial\bar{S}}{\partial t}dAdt=-\int_0^{t_f}\int_{\Omega}\tilde{S}\frac{\partial\bar{S}}{\partial t}dAdt \tag{2.31}$$

Then Eq.(2.29) can be rearranged as:

$$
\begin{aligned}
D_{\Delta f}E(f) = &\frac{1}{Le}\int_0^{t_f}\int_{C_a}\frac{\partial\bar{S}}{\partial n}\Delta f\,dl\,dt+\int_0^{t_f}\int_{\Omega}\tilde{\psi}\left\{\nabla^2\bar{\psi}-J(T,\bar{T})-J(S,\bar{S})\right\}dAdt\\
&+\int_0^{t_f}\int_{\Omega}\tilde{T}\left\{-\frac{\partial\bar{T}}{\partial t}-\nabla\cdot\left(\mathbf{u}\bar{T}+\nabla\bar{T}\right)+Ra_T\,\nabla_n\times(\bar{\psi}\hat{\mathbf{g}})\right\}dAdt\\
&+\int_0^{t_f}\int_{\Omega}\tilde{S}\left\{-\varepsilon\frac{\partial\bar{S}}{\partial t}-\nabla\cdot\left(\mathbf{u}\bar{S}+\frac{1}{Le}\nabla\bar{S}\right)+NRa_T\,\nabla_n\times(\bar{\psi}\hat{\mathbf{g}})+(S-S_m)\sum_{i=1}^{n}\delta(\vec{r}-\vec{r}_i)\right\}dAdt
\end{aligned}
\tag{2.32}
$$

In order to obtain the minimum values, we require that all the terms in brackets of Eq.(2.32) are equal to zero. Then it gives the adjoint equations:

$$\nabla^2\overline{\psi} = \frac{\partial(T,\overline{T})}{\partial(x,y)} + \frac{\partial(S,\overline{S})}{\partial(x,y)} \tag{2.33}$$

$$\frac{\partial\overline{T}}{\partial t} + \nabla\cdot\left(\vec{u}\overline{T} + \nabla\overline{T}\right) = Ra_T\nabla_n\times\left(\overline{\psi}\,\hat{g}\right) \tag{2.34}$$

$$\varepsilon\frac{\partial\overline{S}}{\partial t} + \nabla\cdot\left(\vec{u}\overline{S} + \frac{1}{Le}\nabla\overline{S}\right) = Ra_T N\nabla_n\times\left(\overline{\psi}\,\hat{g}\right) + (S - S_m)\sum_{i=1}^{n}\delta(\vec{r} - \vec{r}_i) \tag{2.35}$$

Now only one term finally remains on the right side of Eq.(2.32), i.e.,

$$D_{\Delta f}E(f) = \frac{1}{Le}\int_0^{t_f}\int_{C_a}\frac{\partial\overline{S}}{\partial n}\Delta f\, dldt \tag{2.36}$$

Comparing Eq. (2.36) with Eq. (2.11), formally

$$\left\langle \nabla E|\Delta f\right\rangle = \left\langle \frac{1}{Le}\frac{\partial\overline{S}}{\partial n}|\Delta f\right\rangle$$

This implies that the gradient of the error is equal to the gradient of adjoint concentration in normal direction on the active boundary, i.e.,

$$\nabla E = \frac{1}{Le}\frac{\partial\overline{S}}{\partial n}\Big|_{C_a} \tag{2.37}$$

Generally this holds true for an arbitrary *f(y ,t)* on the active boundary, irrespective of the shape of the domain or the specific form of the boundary conditions on temperature and concentration.

According to the assumptions drawn in *Page* 33 and the problem definition stated in *Section 1.1*, the boundary conditions for adjoint equations can be summarized as:

$$\overline{\psi}\big|_C = 0$$

$$\overline{T}\big|_{x=0,L} = 0,\ \frac{\partial \overline{T}}{\partial y}\Big|_{y=0,H} = 0$$

$$\overline{S}\big|_{x=0,L} = 0,\ \frac{\partial \overline{S}}{\partial y}\Big|_{y=0,H} = 0$$

2.2.3 Optimization Procedure

Since ∇E and other necessary information can be obtained by solving the sensitivity and adjoint equations, there are no more difficulties to apply the conjugate gradient method in inverse problems.

The overall iterative CGM (Polak-Ribiere version) algorithm may be summarized as follows:

1. Set initial guess $f^{(0)} = 0$, set iteration counter $k = 0$;

2. Solve the direct problem with $f^{(k)}$ to obtain $S^{(k)}$ at the sensors;

3. Evaluate the difference $S^{(k)} - S_m$ at the sensors;

4. Solve the adjoint problem backward in time for $\overline{S}^{(k)}$;

5. Evaluate the gradient of error according to Eq.(2.37) at the active boundary;

6. Calculate the search direction P^k:

$$P^k = \begin{cases} -\nabla E^{(k)} & if \quad k = 0 \\ -\nabla E^{(k)} + \beta^k P^{k-1} & if \quad k > 0 \end{cases} \tag{2.38}$$

where

$$\beta^k = \frac{\left\langle \nabla E^{(k)} - \nabla E^{(k-1)} \middle| \nabla E^{(k)} \right\rangle}{\left\| \nabla E^{(k-1)} \right\|^2} \tag{2.39}$$

7. Solve the sensitivity problem with $\Delta f = P^k$ at x = 0 to obtain $\tilde{S}^{(k)}$ at the sensors;

8. Calculate the step size

$$\alpha^k = -\frac{\left\langle S^{(k)} - S_m \middle| \tilde{S}^{(k)} \right\rangle}{\left\| \tilde{S}^{(k)} \right\|^2} \tag{2.40}$$

9. Update to $f^{(k+1)} = f^{(k)} + \alpha^k P^k$;

10. Set $k = k + 1$, go back to step 2, repeat until convergence criterion $E^{(k)} < \varepsilon E_0$ is satisfied.

The discrepancy principle of Alifanov can be used to select the value for ε when the measured data contain uniformly distributed random errors. The convergence criterion $\varepsilon = \sigma^2$ can be easily obtained by Eq.(2.1) and the assumption $S^{(k)}$-$S_m \approx \sigma S_m$. For the case of exact measured data however, the stopping criterion is set at $\varepsilon = 2.5 \times 10^{-5}$ for all the results presented in this thesis. The solutions of α, β, and E are numerically evaluated by Simpson's method.

CHAPTER III
NUMERICAL IMPLEMENTATION

For the direct problem, the sensitivity problem and the adjoint problem, all the equation groups have been closed. Theoretically speaking, the solutions should be obtained. As we known, it is impossible to get exact solutions for all of the partial differential equations. It depends on the boundary conditions, the shape of the system, and the equations themselves. However, approximate solutions may always be achieved by numerical techniques.

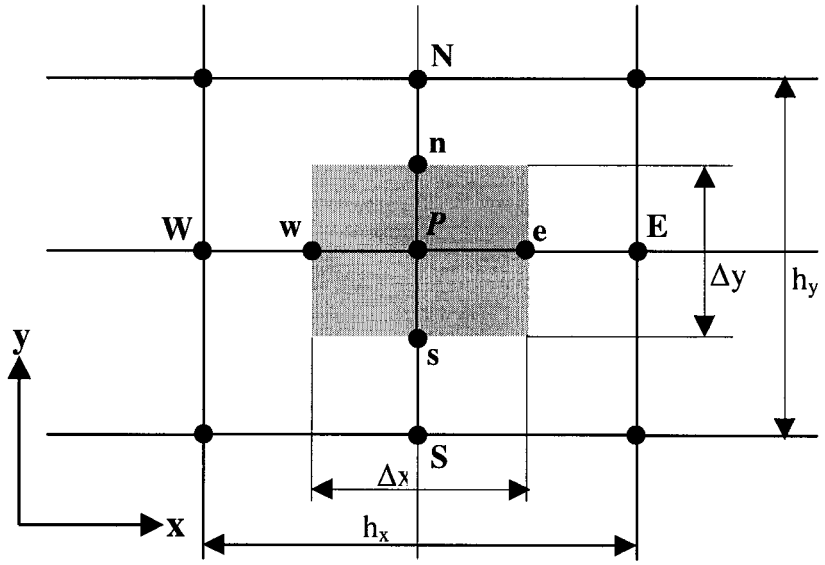

Fig. 3.1 Control Volume of 2-D Problem

The numerical methods usually require the objective equations to be discretized. The most popular discretizaton methods perhaps are *finite difference* which is based on the Taylor series expansion and *finite element* which is based on the principles of variation or weighted residuals. In this study, *control volume method* [41] which is based on the integral equilibrium of control volume is used due to its advantage which has been proved by numerous applications to heat transfer problems in a system with regular geometry. Additionally, completely implicit form is also adopted to ensure the stability

of iterative computation. The control volume used in a two-dimensional problem is as shown in Fig.2.1, we set $h_x = 2\Delta x$ and $h_y = 2\Delta y$ in this study.

3.1 Discretization of Governing Equations

3.1.1 Discretization of Non-Dimensional Energy Equation

Considering the continuity equation, the non-dimensional energy equation namely Eq.(1.40) also can be written in the following conservative form:

$$\frac{\partial T}{\partial t}+\frac{\partial}{\partial x}\left(uT-\frac{\partial T}{\partial x}\right)+\frac{\partial}{\partial y}\left(vT-\frac{\partial T}{\partial y}\right)=0 \tag{3.1}$$

If we define:

$$J_x = uT-\frac{\partial T}{\partial x} \tag{3.2}$$

$$J_y = vT-\frac{\partial T}{\partial y} \tag{3.3}$$

then Eq. (3.1) becomes:

$$\frac{\partial T}{\partial t}+\frac{\partial J_x}{\partial x}+\frac{\partial J_y}{\partial y}=0 \tag{3.4}$$

Integrating Eq. (3.4) over control volume, we can get:

$$\frac{T_P-T_P^0}{\Delta t}\Delta x\Delta y + J_e - J_w + J_n - J_s = 0 \tag{3.5}$$

where $J_e = \int J_x dy = u_e T_e \Delta y - \frac{(T_E - T_P)\Delta y}{\Delta x}$ (3.6a)

$$J_w = \int J_x dy = u_w T_w \Delta y - \frac{(T_P - T_W)\Delta y}{\Delta x} \tag{3.6b}$$

$$J_n = \int J_y dx = u_n T_n \Delta x - \frac{(T_N - T_P)\Delta x}{\Delta y} \tag{3.6c}$$

$$J_s = \int J_y dx = u_s T_s \Delta x - \frac{(T_P - T_W)\Delta x}{\Delta y} \tag{3.6d}$$

The non-dimensional continuity equation, namely $\frac{\partial u}{\partial x}+\frac{\partial v}{\partial y}=0$, can be discretized in the same way as follow:

$$F_e - F_w + F_n - F_s = 0 \tag{3.7}$$

where $F_e = u_e \Delta y$ (3.8a)

$$F_w = u_w \Delta y \tag{3.8b}$$

$$F_n = v_n \Delta x \tag{3.8c}$$

$$F_s = v_s \Delta x \tag{3.8d}$$

Eq. (3.5) – Eq. (3.7)*T_p, we have

$$\frac{T_P - T_P^0}{\Delta t}\Delta x \Delta y + \left(J_e - F_e T_P\right) - \left(J_w - F_w T_P\right) + \left(J_n - F_n T_P\right) - \left(J_s - F_s T_P\right) = 0 \tag{3.9}$$

We now rewrite Eq.(3.9) as following standard form:

$$a_P T_P = a_E T_E + a_W T_W + a_N T_N + a_S T_S + b \tag{3.10}$$

Where $a_E = D_e A\left(\left|(Pe)_e\right|\right) + Max(-F_e, 0)$

$$a_W = D_w A\left(\left|(Pe)_w\right|\right) + Max(F_w, 0)$$

$$a_N = D_n A\left(\left|(Pe)_n\right|\right) + Max(-F_n, 0)$$

$$a_S = D_s A\left(\left|(Pe)_s\right|\right) + Max(F_s, 0)$$

$$a_P = a_E + a_W + a_N + a_S + \frac{\Delta x \Delta y}{\Delta t}$$

$$b = \frac{\Delta x \Delta y T_P^0}{\Delta t}$$

and:

$$D_e = D_w = \frac{\Delta y}{\Delta x}$$

$$D_n = D_s = \frac{\Delta x}{\Delta y}$$

The Peclet Number is defined as:

$$Pe = \frac{F}{D}$$

so:

$$(Pe)_e = u_e \Delta x$$

$$(Pe)_w = u_w \Delta x$$

$$(Pe)_n = u_n \Delta y$$

$$(Pe)_s = u_s \Delta y$$

Scheme	Expression of $A(\|Pe\|)$
Central difference	$1-0.5\|Pe\|$
Upwind	1
Mixed format	$Max[0,(1-0.5\|Pe\|)]$
Power law	$Max[0,(1-0.1\|Pe\|)^5]$
Exponent format	$\|Pe\|/[exp(\|Pe\|)-1]$

Table 3.1 The Different Expressions for Function $A(|Pe|)$

There are at least five methods that can be used to calculate the function $A(|Pe|)$ shown in Table 3.1. Compared with central difference, upwind format and mixed format, the so-called *power law scheme* namely Eq.(3.11) which was proposed by Patankar may achieve the physically real and relatively precise solutions even for very large Peclet

number as well as strong convection. So, in this study, power law scheme is chosen to perform numerical calculations.

$$A(|Pe|) = Max\left[0,(1-0.1|Pe|)^5\right] \tag{3.11}$$

Lastly, it is must be pointed out that the velocities u and v are evaluated according to the following discrete equation:

$$u_P = \frac{\psi_E - \psi_W}{2\Delta x}, \quad v_P = -\frac{\psi_N - \psi_S}{2\Delta y} \tag{3.12}$$

3.1.2 Discretization of Non-Dimensional Mass Diffusion Equation

In the same way, we may rewrite the non-dimensional energy equation namely Eq.(1.41) as:

$$\varepsilon\frac{\partial S}{\partial t} + \frac{\partial}{\partial x}\left(uS - \frac{1}{Le}\frac{\partial S}{\partial x}\right) + \frac{\partial}{\partial y}\left(vS - \frac{1}{Le}\frac{\partial S}{\partial y}\right) = 0 \tag{3.13}$$

We find this equation similar to Eq.(3.1), so the discrete equation can be obtained directly:

$$a_P S_P = a_E S_E + a_W S_W + a_N S_N + a_S S_S + b \tag{3.14}$$

Where $a_E = D_e A(|(Pe)_e|) + Max(-F_e, 0)$

$$a_W = D_w A(|(Pe)_w|) + Max(F_w, 0)$$

$$a_N = D_n A(|(Pe)_n|) + Max(-F_n, 0)$$

$$a_S = D_s A(|(Pe)_s|) + Max(F_s, 0)$$

$$a_P = a_E + a_W + a_N + a_S + \varepsilon\frac{\Delta x \Delta y}{\Delta t}$$

$$b = \varepsilon\frac{\Delta x \Delta y S_P^0}{\Delta t}$$

$$D_e = D_w = \frac{1}{Le}\frac{\Delta y}{\Delta x}$$

$$D_n = D_s = \frac{1}{Le}\frac{\Delta x}{\Delta y}$$

$$F_e = u_e \Delta y$$

$$F_w = u_w \Delta y$$

$$F_n = v_n \Delta x$$

$$F_s = v_s \Delta x$$

$$(Pe)_e = u_e \Delta x Le$$

$$(Pe)_w = u_w \Delta x Le$$

$$(Pe)_n = u_n \Delta y Le$$

$$(Pe)_s = u_s \Delta y Le$$

3.1.3 Discretization of Non-Dimensional Stream Function Equation

Non-dimensional stream function equation in 2-D Cartesian coordinates is as follow:

$$\frac{\partial^2 \psi}{\partial x^2} + \frac{\partial^2 \psi}{\partial y^2} = Ra_T \left(\frac{\partial T}{\partial x} + N \frac{\partial S}{\partial x} \right)$$

Calculate the integral of this equation in control volume, namely

$$Ra_T \int_s^n \int_w^e \left(\frac{\partial T}{\partial x} + N \frac{\partial S}{\partial x} \right) dxdy = \int_s^n \int_w^e \left(\frac{\partial^2 \psi}{\partial x^2} + \frac{\partial^2 \psi}{\partial y^2} \right) dxdy \tag{3.15}$$

we have

$$Ra_T \left(\frac{T_E - T_W}{2} + N \frac{S_E - S_W}{2} \right) \Delta y = \left(\frac{\psi_E - \psi_P}{\Delta x} - \frac{\psi_P - \psi_W}{\Delta x} \right) \Delta y + \left(\frac{\psi_N - \psi_P}{\Delta y} - \frac{\psi_P - \psi_S}{\Delta y} \right) \Delta x \tag{3.16}$$

We transform Eq. (3.16) to standard discrete form:

$$\left(\frac{2\Delta y}{\Delta x}+\frac{2\Delta x}{\Delta y}\right)\psi_P=\frac{\Delta y}{\Delta x}\psi_E+\frac{\Delta y}{\Delta x}\psi_W+\frac{\Delta x}{\Delta y}\psi_N+\frac{\Delta x}{\Delta y}\psi_S-Ra_T\left(\frac{T_E-T_W}{2}+N\frac{S_E-S_W}{2}\right)\Delta y$$

or

$$A_P\psi_P=A_E\psi_E+A_W\psi_W+A_N\psi_N+A_S\psi_S+B \tag{3.17}$$

where,

$$A_E=A_W=\frac{\Delta y}{\Delta x}$$

$$A_N=A_S=\frac{\Delta x}{\Delta y}$$

$$A_P=A_E+A_W+A_N+A_S$$

$$B=-Ra_T\left(\frac{T_E-T_W}{2}+N\frac{S_E-S_W}{2}\right)\Delta y$$

3.2 Discretization of Sensitivity Equations

The sensitivity stream function equation is same as the direct stream function equation if the variables $\tilde{\psi}$, $\tilde{T}$ and $\tilde{S}$ are replaced by ψ, T and S. Naturally the discretization of former need not be repeated again.

The sensitivity temperature equation and the sensitivity concentration equation are similar, so we only discuss the one of them for its discretization.

For the sensitivity temperature equation, namely

$$\frac{\partial\tilde{T}}{\partial t}+\nabla\cdot\left(\tilde{\vec{u}}T\right)+\nabla\cdot\left(\vec{u}\tilde{T}\right)=\nabla^2\tilde{T},$$

the big problem is how to treat the second term and third term on the left hand side of this equation. There is no verdict for this problem so far. In my opinion, the second term should be regarded as "source term" and be discretized using central difference method, and the third term can be treated as "convection term". Based on this assumption, we rewrite the sensitivity temperature equation:

$$\frac{\partial \tilde{T}}{\partial t}+\frac{\partial}{\partial x}\left(u\tilde{T}-\frac{\partial \tilde{T}}{\partial x}\right)+\frac{\partial}{\partial y}\left(v\tilde{T}-\frac{\partial \tilde{T}}{\partial y}\right)=-\left[\frac{\partial(\tilde{u}T)}{\partial x}+\frac{\partial(\tilde{v}T)}{\partial y}\right] \tag{3.18}$$

By virtue of the control volume method, we can easily derive the discrete equation from Eq.(3.18):

$$a_P\tilde{T}_P = a_E\tilde{T}_E + a_W\tilde{T}_W + a_N\tilde{T}_N + a_S\tilde{T}_S + b \tag{3.19}$$

Where $a_E = D_e A(|(Pe)_e|) + Max(-F_e, 0)$

$$a_W = D_w A(|(Pe)_w|) + Max(F_w, 0)$$

$$a_N = D_n A(|(Pe)_n|) + Max(-F_n, 0)$$

$$a_S = D_s A(|(Pe)_s|) + Max(F_s, 0)$$

$$a_P = a_E + a_W + a_N + a_S + \frac{\Delta x \Delta y}{\Delta t}$$

$$b = \frac{\Delta x \Delta y \tilde{T}_P^0}{\Delta t} - [(\tilde{u}_e T_e - \tilde{u}_w T_w)\Delta y + (\tilde{u}_n T_n - \tilde{u}_s T_s)\Delta x]$$

$$D_e = D_w = \frac{\Delta y}{\Delta x}$$

$$D_n = D_s = \frac{\Delta x}{\Delta y}$$

$$F_e = u_e \Delta y$$

$$F_w = u_w \Delta y$$

$$F_n = v_n \Delta x$$

$$F_s = v_s \Delta x$$

$$(Pe)_e = u_e \Delta x$$

$$(Pe)_w = u_w \Delta x$$

$$(Pe)_n = u_n \Delta y$$

$$(Pe)_s = u_s \Delta y$$

3.3 Discretization of Adjoint Equations

❖ Discretization of Adjoint Stream Function Equation

Just as for the discretization of stream function equation, calculating the integrals of the two side of adjoint stream function equation namely Eq.(2.33) at first, we have:

$$\left(\frac{\overline{\psi}_E - \overline{\psi}_P}{\Delta x} - \frac{\overline{\psi}_P - \overline{\psi}_W}{\Delta x}\right)\Delta y + \left(\frac{\overline{\psi}_N - \overline{\psi}_P}{\Delta y} - \frac{\overline{\psi}_P - \overline{\psi}_S}{\Delta y}\right)\Delta x =$$
$$\left(\frac{\overline{T}_E - \overline{T}_W}{2\Delta x}\frac{\overline{T}_N - \overline{T}_S}{2\Delta y} - \frac{T_E - T_W}{2\Delta x}\frac{T_N - T_S}{2\Delta y}\right)\Delta x\Delta y + \left(\frac{\overline{S}_E - \overline{S}_W}{2\Delta x}\frac{\overline{S}_N - \overline{S}_S}{2\Delta y} - \frac{S_E - S_W}{2\Delta x}\frac{S_N - S_S}{2\Delta y}\right)\Delta x\Delta y \tag{3.20}$$

Rearranging the terms of Eq.(3.20), we obtain the standard form:

$$\left(\frac{2\Delta y}{\Delta x} + \frac{2\Delta x}{\Delta y}\right)\overline{\psi}_P = \frac{\Delta y}{\Delta x}\overline{\psi}_E + \frac{\Delta y}{\Delta x}\overline{\psi}_W + \frac{\Delta x}{\Delta y}\overline{\psi}_N + \frac{\Delta x}{\Delta y}\overline{\psi}_S$$
$$+\left(\frac{(T_E - T_W)(T_N - T_S)}{4} - \frac{(\overline{T}_E - \overline{T}_W)(\overline{T}_N - \overline{T}_S)}{4}\right)$$
$$+\left(\frac{(S_E - S_W)(S_N - S_S)}{4} - \frac{(\overline{S}_E - \overline{S}_W)(\overline{S}_N - \overline{S}_S)}{4}\right)$$

or

$$A_P\overline{\psi}_P = A_E\overline{\psi}_E + A_W\overline{\psi}_W + A_N\overline{\psi}_N + A_S\overline{\psi}_S + B \tag{3.21}$$

where,

$$A_E = A_W = \frac{\Delta y}{\Delta x}$$

$$A_N = A_S = \frac{\Delta x}{\Delta y}$$

$$A_P = A_E + A_W + A_N + A_S$$

$$B = \left(\frac{(T_E - T_W)(T_N - T_S)}{4} - \frac{(\overline{T}_E - \overline{T}_W)(\overline{T}_N - \overline{T}_S)}{4} \right) + \left(\frac{(S_E - S_W)(S_N - S_S)}{4} - \frac{(\overline{S}_E - \overline{S}_W)(\overline{S}_N - \overline{S}_S)}{4} \right)$$

❖ Discretization of Adjoint Temperature and Concentration Equation

Comparing adjoint temperature equation with adjoint concentration equation, one might find these two very similar, except that the latter contains one more source term namely $S - S_m$. In order to avoid poll-parroting, we only introduce the discretization of adjoint temperature equation namely:

$$\frac{\partial \overline{T}}{\partial t} + \frac{\partial}{\partial x}\left(u\overline{T} + \frac{\partial \overline{T}}{\partial x} \right) + \frac{\partial}{\partial y}\left(v\overline{T} + \frac{\partial \overline{T}}{\partial y} \right) = Ra_T \frac{\partial \overline{\psi}}{\partial x} \tag{3.22}$$

The general equation of 2-D convection and diffusion might be written as:

$$\frac{\partial \phi}{\partial t} + \frac{\partial}{\partial x}\left(u\phi - \Gamma \frac{\partial \phi}{\partial x} \right) + \frac{\partial}{\partial y}\left(v\phi - \Gamma \frac{\partial \phi}{\partial y} \right) = S \tag{3.23}$$

where ϕ is any parameter, Γ is called coefficient of diffusion ($\Gamma > 0$), and S stands for source term.

Obviously the diffusive coefficient of Eq.(3.22) is negative. If it could become positive, we may easily get the familiar discrete equation form which has been tested by mathematical theory and numerical practice. For this purpose, we define a new time variable τ instead of the real physical time t [4]:

$$\tau = t_f - t \tag{3.24}$$

Then $d\tau = -dt$ and Eq.(3.23) becomes:

$$\frac{\partial \overline{T}}{\partial \tau} + \frac{\partial}{\partial x}\left((-u)\overline{T} - \frac{\partial \overline{T}}{\partial x}\right) + \frac{\partial}{\partial y}\left((-v)\overline{T} - \frac{\partial \overline{T}}{\partial y}\right) = -Ra_T \frac{\partial \overline{\psi}}{\partial x} \tag{3.25}$$

Via this transformation, the adjoint problem becomes an initial value problem in τ with a positive diffusive coefficient which brings stability during computation. In addition, since all the adjoint parameters are equal to zero at $t = t_f$, then $f^{(k)}(t_f) \equiv f^{(0)}(t_f)$. Therefore a realistic guess is required at $\tau = 0$ $(t = t_f)$ otherwise the convergence may be very slow [42].

Based on Eq.(3.25), it is straightforward to get the discrete equation of adjoint temperature considering the discussion in *Section 3.1.1*:

$$a_P \overline{T}_P = a_E \overline{T}_E + a_W \overline{T}_W + a_N \overline{T}_N + a_S \overline{T}_S + b \tag{3.26}$$

Where $a_E = D_e A(|(Pe)_e|) + Max(-F_e, 0)$

$$a_W = D_w A(|(Pe)_w|) + Max(F_w, 0)$$

$$a_N = D_n A(|(Pe)_n|) + Max(-F_n, 0)$$

$$a_S = D_s A(|(Pe)_s|) + Max(F_s, 0)$$

$$a_P = a_E + a_W + a_N + a_S + \frac{\Delta x \Delta y}{\Delta t}$$

$$b = \frac{\Delta x \Delta y \overline{T}_P^0}{\Delta t} - Ra_T(\overline{\psi}_e - \overline{\psi}_w)\Delta y$$

$$D_e = D_w = \frac{\Delta y}{\Delta x}$$

$$D_n = D_s = \frac{\Delta x}{\Delta y}$$

$$F_e = -u_e \Delta y$$

$$F_w = -u_w \Delta y$$

$$F_n = -v_n \Delta x$$

$$F_s = -v_s \Delta x$$

$$(Pe)_e = -u_e \Delta x$$

$$(Pe)_w = -u_w \Delta x$$

$$(Pe)_n = -u_n \Delta y$$

$$(Pe)_s = -u_s \Delta y$$

3.4 Grids and Line-by-line Iterative Method

In order to propagate the boundary information to the inner nodes faster, the so-called line-by-line method is adopted to perform the iterative calculation by sweeping the line and column alternating from left to right and from bottom to top at each time step. Also, the iterative computations on a given line or two column are achieved by Gauss—Seidel method. On the other hand, under-relaxation coefficients ξ are used to prevent the divergence of results.

For a rectangular system, we usually prefer the uniform grids as shown in FIG. 3.2: a square is divided into 400 equal grids. Mathematically speaking, one may get more accurate solutions through uniform grids. However, for some cases such as when the convection is very strong or/and the boundary layer is very thin, i.e., the gradient of temperature and concentration in the area near the boundaries is very large, we need smaller mesh to obtain physically realistic results. We can certainly increase the number of nodes. The other way, for the sake of saving calculation time, is to choose the non-uniform grids as shown in FIG. 3.3a and FIG. 3.3b.

The coefficients of mesh *CMX* and *CMY* are defined as follows:

$$\begin{cases} x(i) = \frac{1}{2}\left(\frac{i-1}{i_{MAX}-1}\right)^{CMX} & 1 \le i \le i_{MAX}\ ; \\ x(2i-1) = 1 - x(i) \end{cases}$$

$$\begin{cases} y(j) = \frac{1}{2}\left(\frac{j-1}{j_{MAX}-1}\right)^{CMY} & 1 \le j \le j_{MAX} \\ y(2j-1) = 1 - y(j) \end{cases}$$

where x and y are the position of the nodes.

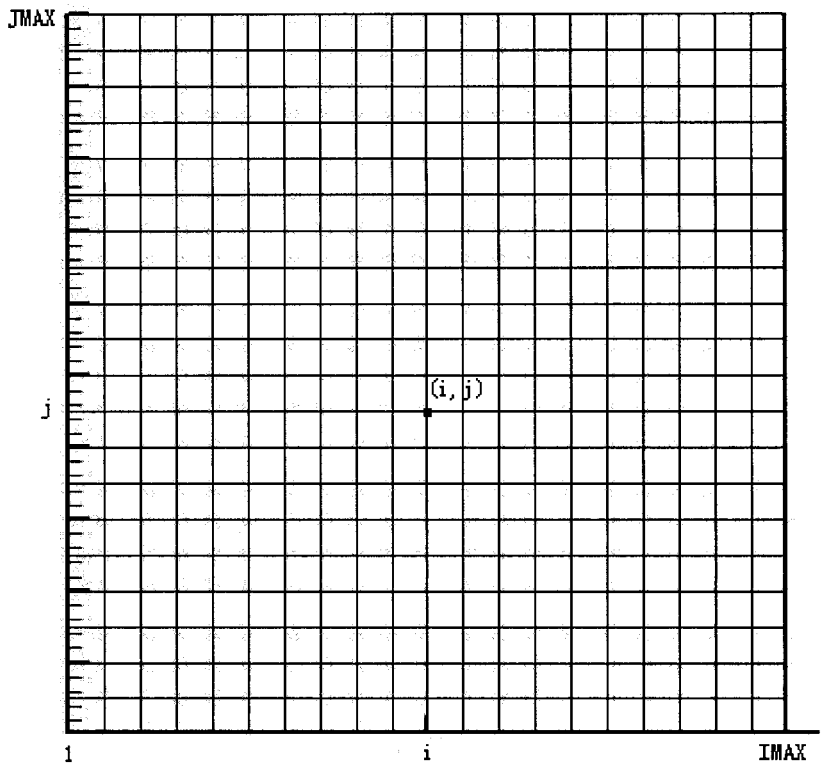

Figure 3.2 Uniform 21×21 Grids

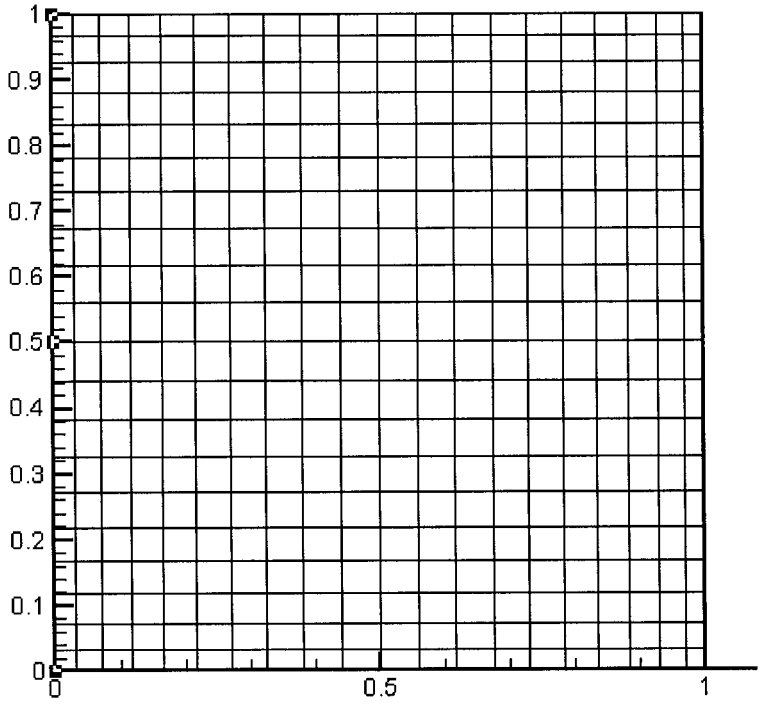

Figure 3.3a Non-uniform 21×21 Grids (CMX=1.2, CMY=1.2)

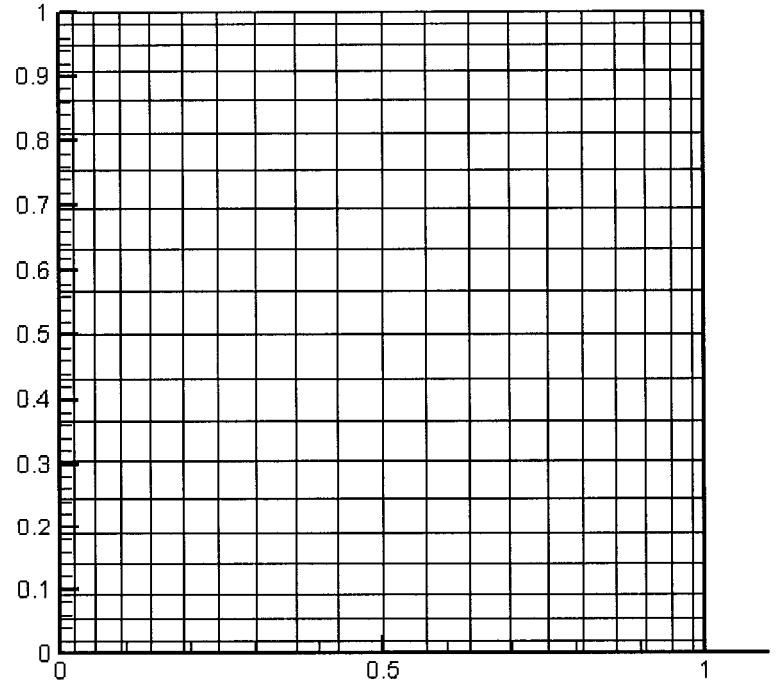

Figure 3.3b Non-uniform 21×21 Grids (CMX=1.4, CMY=1.4)

CHAPTER IV
RESULTS AND DISCUSSION

The direct, sensitivity and adjoint equations are solved by the numerical method discussed in Chapter III. The results for different cases are presented in this chapter. Because the direct problem is not our main objective of this study, we focus on the inverse problem. At first solutions are presented for an unknown uniform solute concentration profile on active wall. And then the results for non-uniform profile will be introduced.

4.1 Results for Uniform Concentration Profile on Active Boundary

Let us first consider the cases for a concentration profile on the active boundary that is only a function of time, i.e., $S = f(t)$. In this case the solution algorithm requires a small modification, in that the averaged right-hand side of Eq.(2.37) over the active boundary must be used as the error gradient. Obviously, the direct solutions and the inverse solutions should depend on the four closure coefficients namely Rayleigh number, Lewis number, N and ε as well as boundary conditions. In practice, the measured data sometimes is not precise; the error always can't be completely avoided. As we know, even a small error may be fatal for an ill-posed inverse problem. So it is absolutely necessary to test our solution algorithm with noisy data which is used to simulate the real measured values. For the case $S = f(t)$, only one sensor is embedded at the middle of height in the square enclosure because it is known that more sensors cannot lead to any improvement. We will see, however, that the position of sensor is an important factor in solving the inverse problem. To close the direct problem, we suppose the exact concentration at the active boundary is a sine function of time namely $f(t) = \sin(\pi t)$. Most solutions below are based on this assumption. Some other profiles such as line, triangle etc. are also presented as a supplement.

❖ **Effect of Rayleigh Number**

As we discussed above, there are too many factors which can influence the final solutions. For convenience, we vary only one at the time and keep the other ones fixed.

We suppose $Le = N = \varepsilon = 1$, and one sensor is located at the center point namely x=0.5L, y=0.5H.

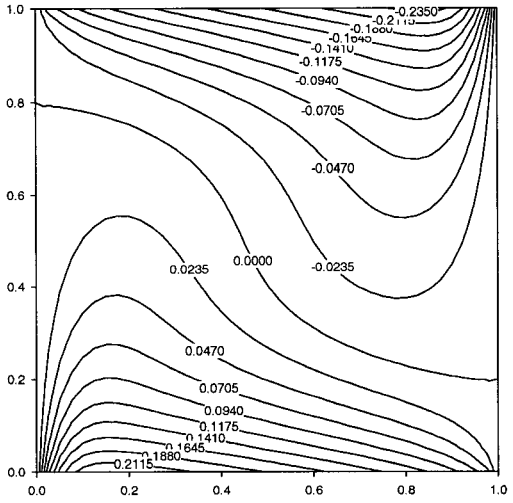

Figure 4.1a Temperature field at $t_f/2$ Ra=100, f(t)=sin(πt)

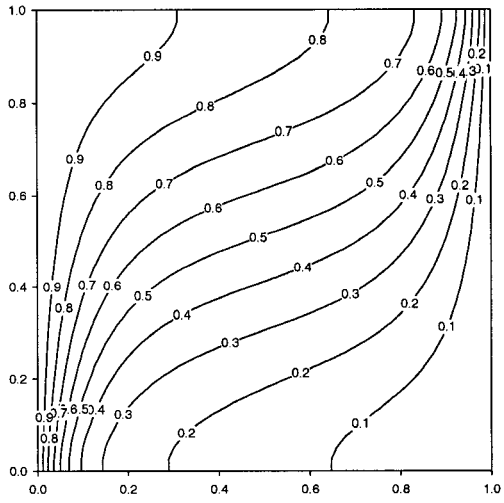

Figure 4.1b Concentration field at $t_f/2$ Ra=100, f(t)=sin(πt)

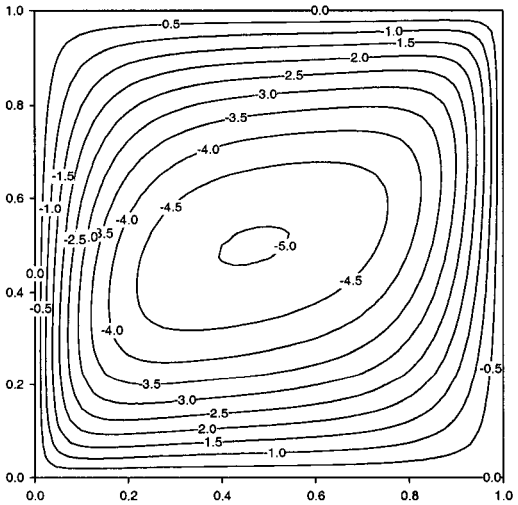

Figure 4.1c Streamline at $t_f/2$, Ra=100, f(t)=sin(πt)

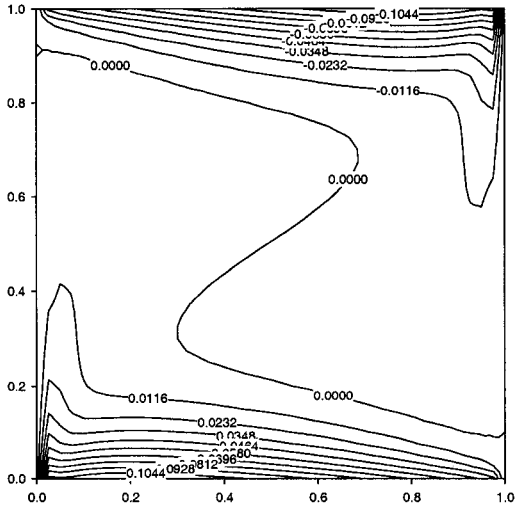

Figure 4.2a Temperature field at $t_f/2$

Ra=1000, f(t)=sin(πt)

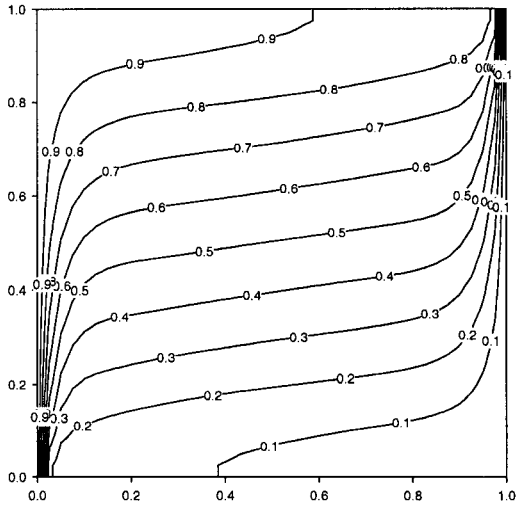

Figure 4.2b Concentration field at $t_f/2$

Ra=1000, f(t)=sin(πt)

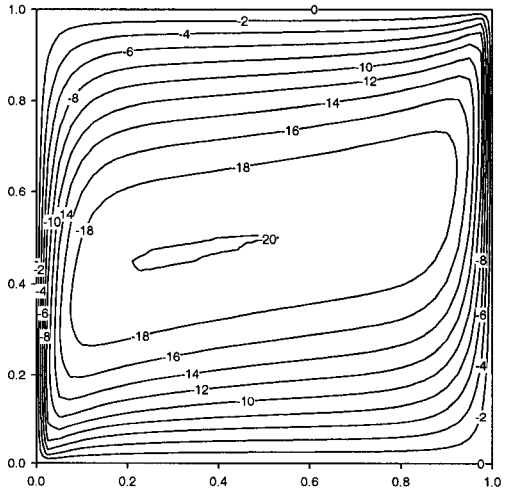

Figure 4.2c Streamline at $t_f/2$, Ra=1000, f(t)=sin(πt)

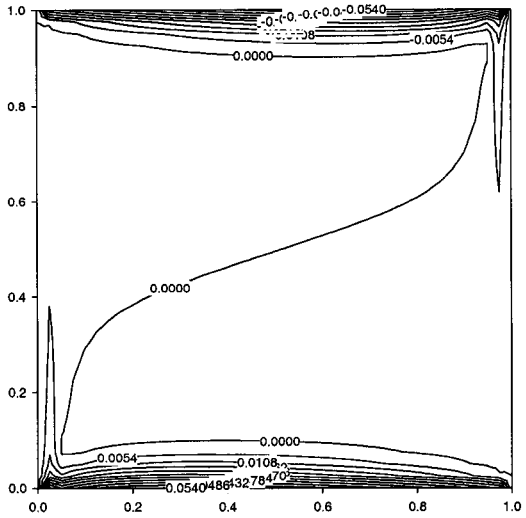

Figure 4.3a Temperature field at $t_f/2$

Ra=10000, f(t)=sin(πt)

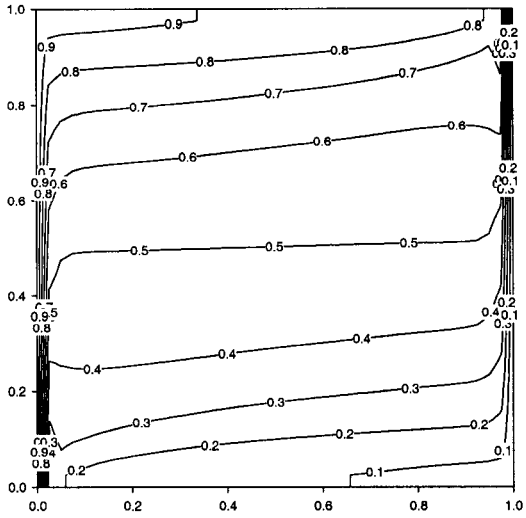

Figure 4.3b Concentration field at $t_f/2$

Ra=10000, f(t)=sin(πt)

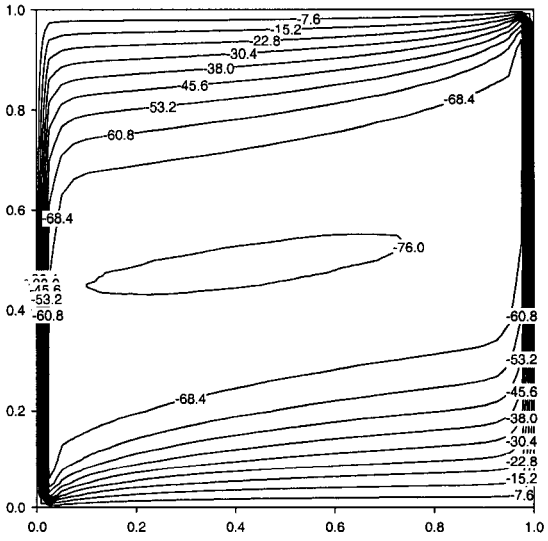

Figure 4.3c Streamline at $t_f/2$, Ra=10000, f(t)=sin(πt)

FIG.4.1~4.3 show the evolution of the direct solutions as Rayleigh number increases. For Ra=100, the convection is relative weak; the gradients of temperature, concentration and stream function within the enclosure are not steep. For Ra=1000 and Ra=10000, the natural convection is strong, and the boundary layer is very thin; the heat transfer only takes place in the small area near the boundary; so finer mesh is needed for solving the direct and inverse problem.

The inverse solution for Ra=100 is presented as shown in FIG. 4.4. Accurate results can be obtained by virtue of 21×21 grids and 7 iterations. The initial guess is set f(t) = 0 at t=0. We found that the first iteration has eliminated the main error, and the result of 3rd iteration was very close to the exact data. One may feel the convergent rate of conjugate gradient method is fast.

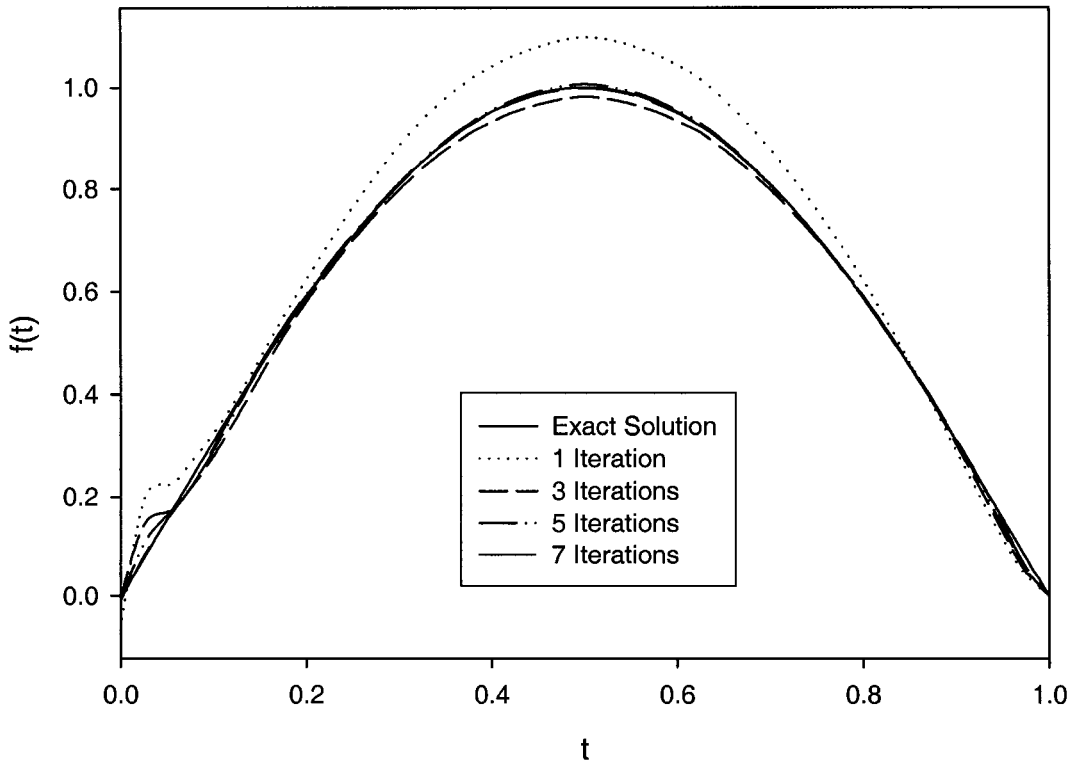

Figure 4.4 Inverse Solution for Concentration f(t) = sin(πt) at x = 0, Ra = 100

For Ra=1000, we must decrease the mesh size to improve the precision, otherwise a reasonable inverse solution can't be obtained. Firstly 21×21 grids are replaced by 41×41 uniform grids. We may also use 21×21 non-uniform grids, setting the coefficients CMX=CMY=1.4. The number of mesh nodes does not change and calculation time is then saved. The comparison between these two ways is shown in FIG. 4.5. For the coarse grid, only 7 iterations are needed, but for the finer, 16 iterations are necessary.

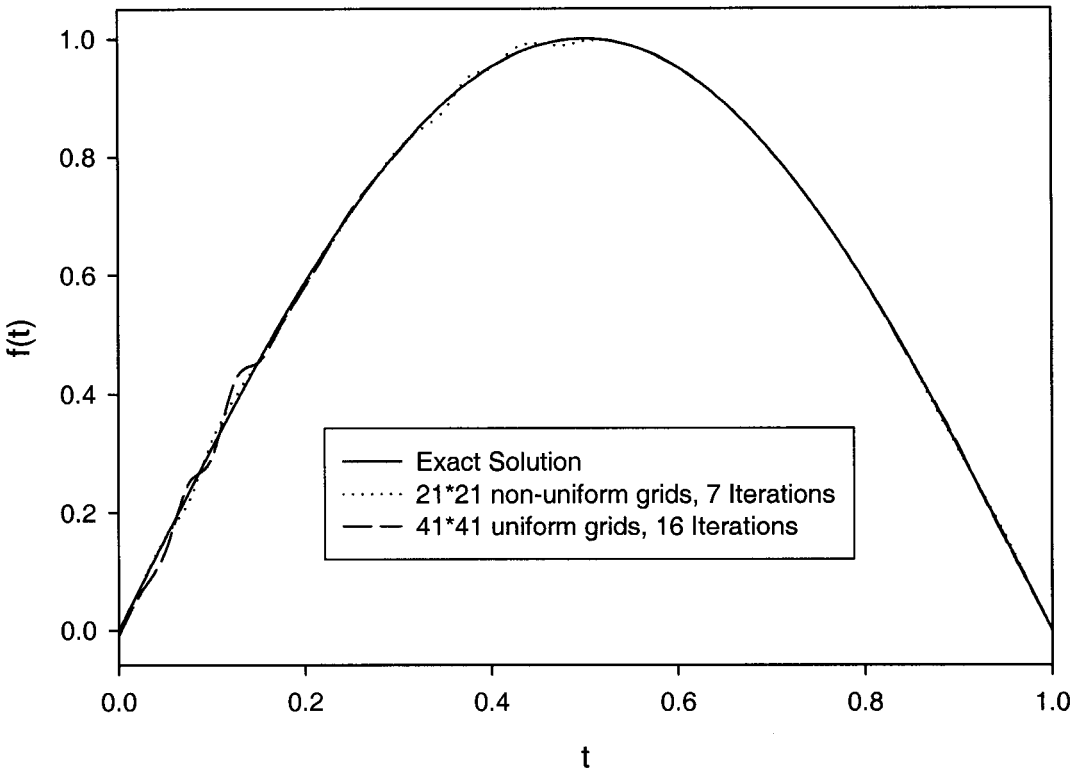

Figure 4.5 Inverse Solution for Concentration f(t) = sin(πt) at x = 0, Ra = 1000

For Ra=10000, the convection is very strong. We have to choose 41×41 non-uniform grids with the coefficient CMX = CMY = 1.4 to make the mesh size small enough in the boundary area. FIG. 4.6 demonstrates the inverse solutions based on the different initial guess. It proves that we can obtain reasonable results for any initial guess f^0. However,

if f^0 is closer to the real value, the inverse solution is better, and less iterations are needed.

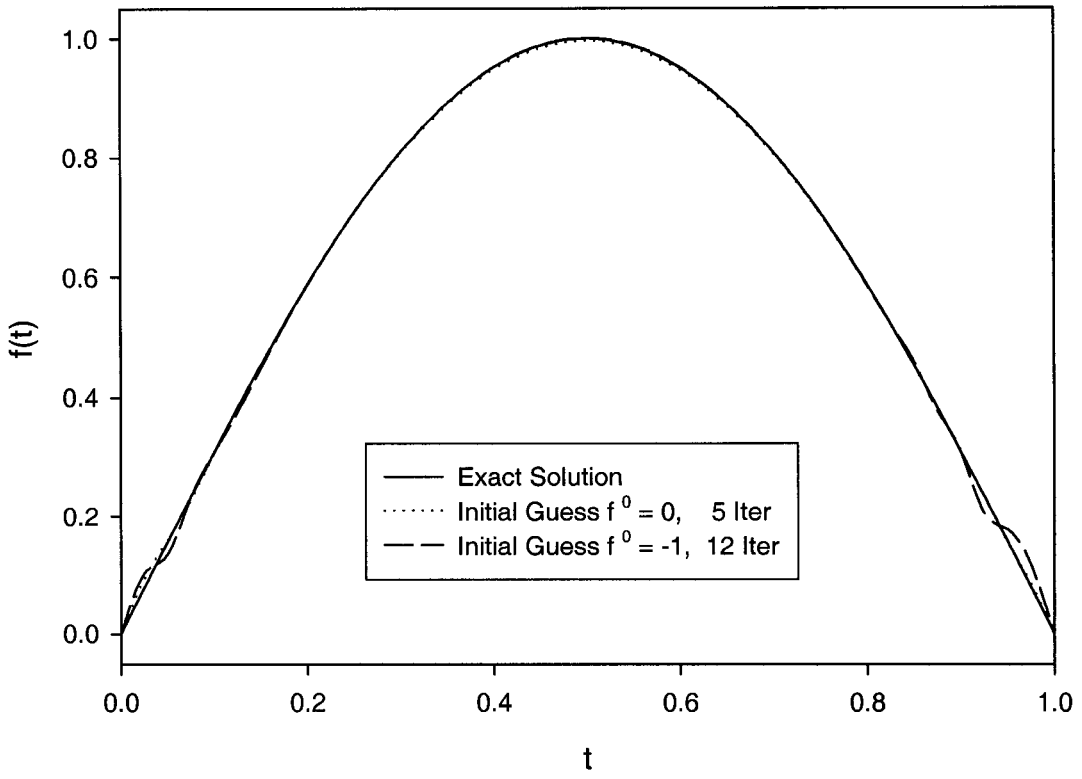

Figure 4.6 Inverse Solution for Concentration f(t) = sin(πt) at x = 0, Ra = 10000

The computations become more and more prone to numerical instability as the Rayleigh number increases further. The adjoint solution as well as sensitivity solution tend to diverge. The sensitivity to the variations on the active boundary also decreases since the convection is so strong. When $Ra>10^5$ there is no way we could achieve the solution except if the sensor is placed closer to the active boundary.

❖ **Effect of Lewis Number, N and ε**

From Eq. (1.39) and the definition of N ratio ($N = \frac{Ra_c}{Ra_T}$), we know the intensity of convection increases as N increases. So increasing the N ratio may lead to divergence even at lower Rayleigh number. When Ra=10000, we can obtain perfect results over the range $0 < N \leq 10$ (see FIG. 4.7).

The ratio $\frac{1}{Le}$ is treated as diffusive coefficient in Eq. (3.13). Obviously if the Lewis number is larger, Peclet number is larger, and the numerical solution is less stable. FIG. 4.8 show that the accuracy of the solution and convergence rate is not influenced much by the Lewis number ranging 0.1 < Le < 5.0. But if Le>5.0, the solution will tend to instability.

In practice, ε is normally ranging between 0.2 and 0.7. Further computations for 0.1 < ε < 1.0 show that the accuracy of the solution is not affected by ε (see FIG. 4.9).

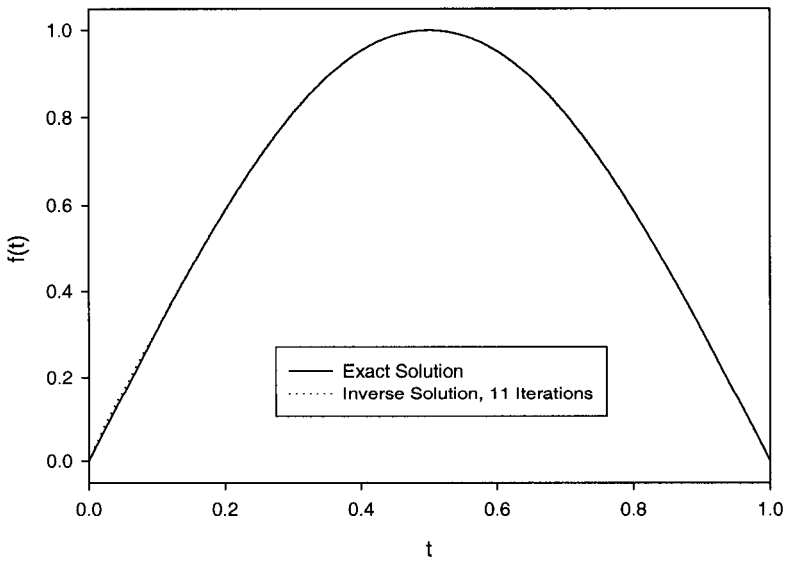

Figure 4.7 Inverse Solution for f(t) = sin(πt) at x = 0

Ra = 10^4, N=10, Le=ε=1

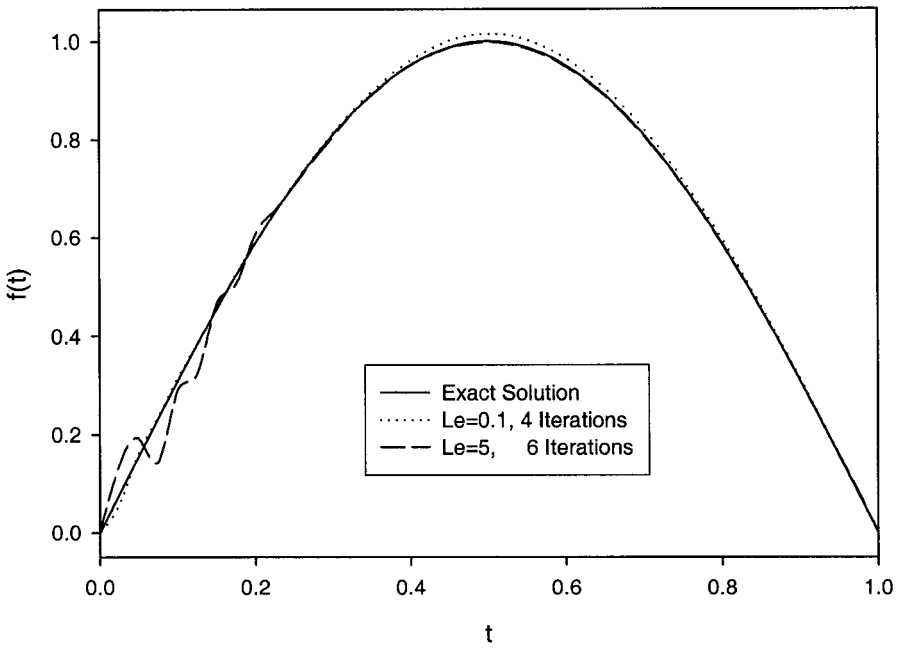

Figure 4.8 Inverse Solution for f(t) = sin(πt) at x = 0, Ra = 10^4, N=ε=1

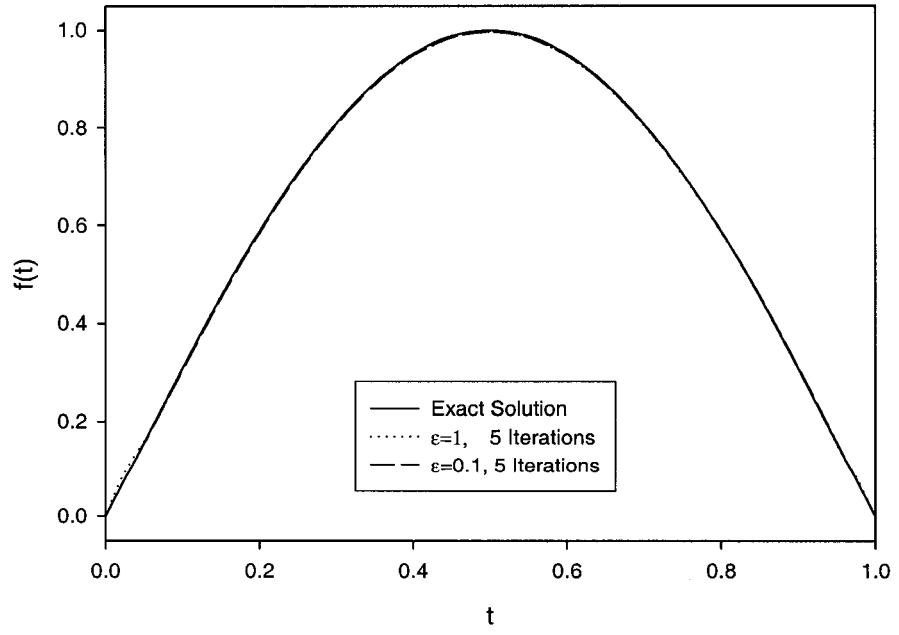

Figure 4.9 Inverse Solution for f(t) = sin(πt) at x = 0, Ra = 10^4, N=Le=1

❖ **Effect of Sensor Position**

In practice, we hope that the sensor can be placed in any position within the system. FIG. 4.10 and FIG. 4.11 show the inverse solutions for different sensor positions. As we expected, when the sensor is placed closer to the active boundary, the accuracy is better and the convergence is faster. Normally, the response of the sensor to the variation of concentration on active boundary is always attenuated and delayed if the sensor is far away from the active wall. Furthermore, in the transfer process of boundary information to sensor point, the numerical error cannot be avoided. Even the mesh size is very small, the truncation error still exists. Anyway, in order to prevent this attenuation of sensitivity, the sensor should be embedded as close as possible to the active boundary.

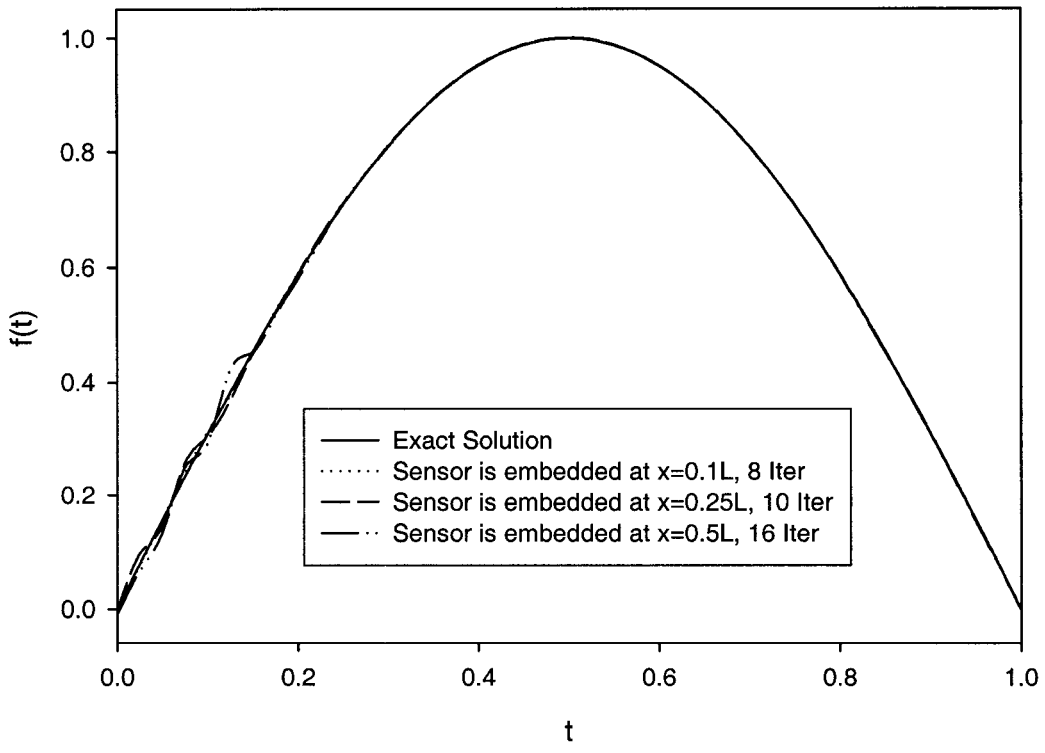

Figure 4.10 Inverse Solution for f(t) = sin(πt) at x = 0, Ra = 10^4, N=Le=ε=1

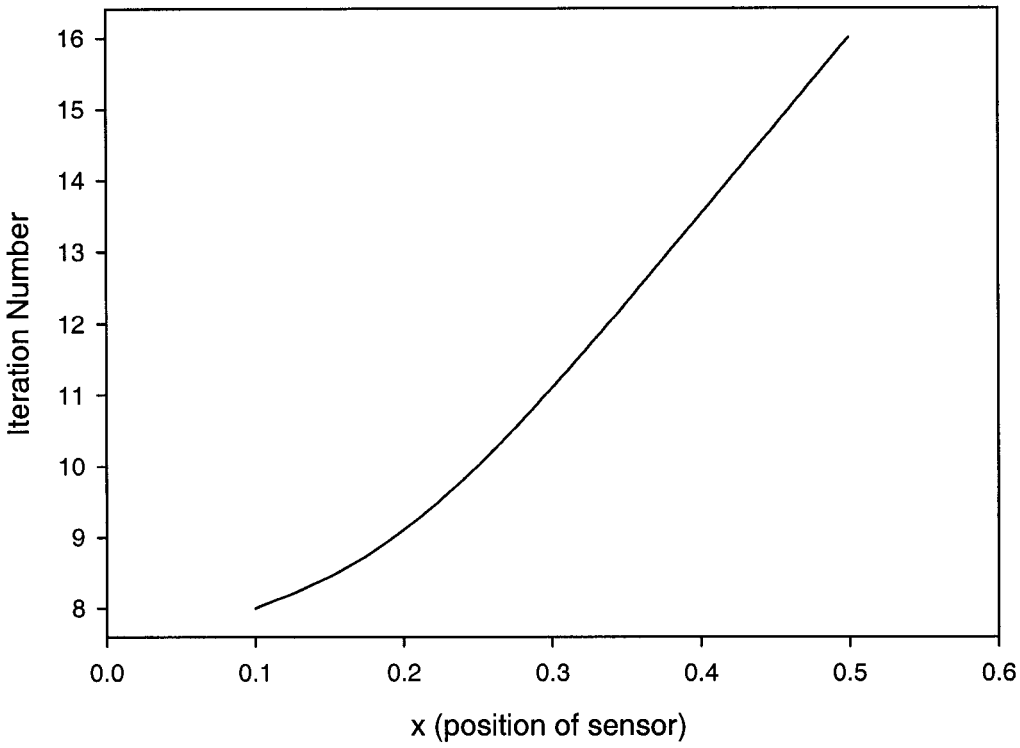

Figure 4.11 Iteration Number vs Sensor Position, Ra = 10^4, N=Le=ε=1

❖ **Different Concentration Profile on Active Boundary**

For the case f(t) = sin(πt) at x = 0, we have obtained perfect results for Rayleigh number at least up to 10000 over parameter ranges $0.1 \le Le < 5$, $0 < N \le 10$ and $0.1 \le \varepsilon \le 1$. FIG.4.12 ~ FIG.4.15 show the solutions for other concentration profiles on active boundary. No matter if triangular or high frequency sinusoidal function profiles are selected, the results are satisfactory at Ra=10000. All the adjoint parameters are equal to zero at $t=t_f$ namely the searching direction $P \equiv 0$ at the initial guess f^0, so $f(t_f)$ must be zero. Then the numerical results in the region near t_f depart from exact values for the case $f(t_f) \neq 0$. FIG.4.16 shows an interesting case where the expected concentration profile is a long pulse. The concentration on the active boundary is discontinuous at t=0.5 and t=1.0. The perfect results obtained in such a case as well as in other cases prove that CGM has good applicability.

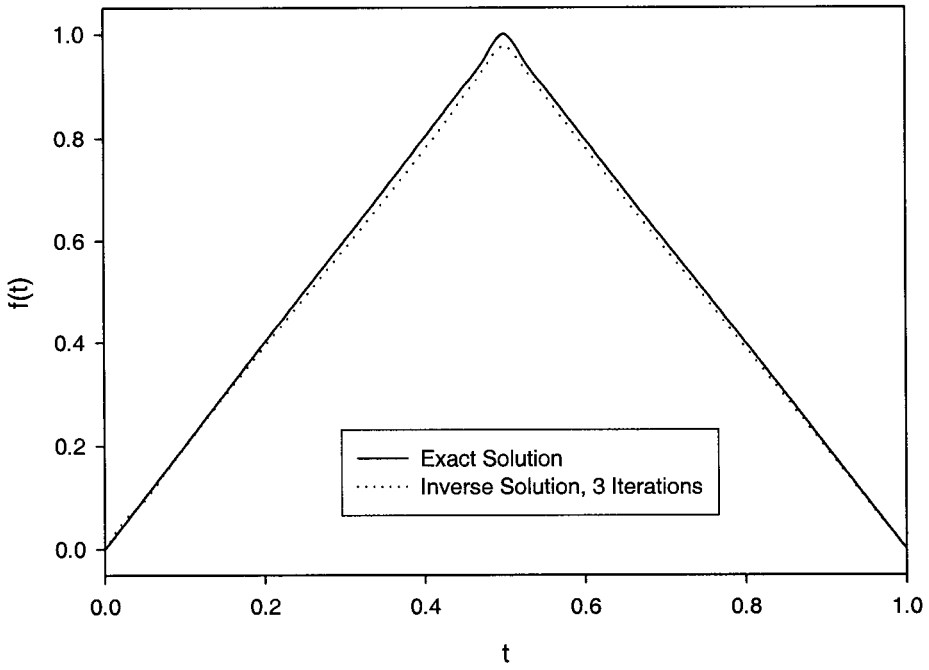

Figure 4.12 Concentration with Triangular Profile at x = 0, Ra = 10^4, N=Le=ε=1

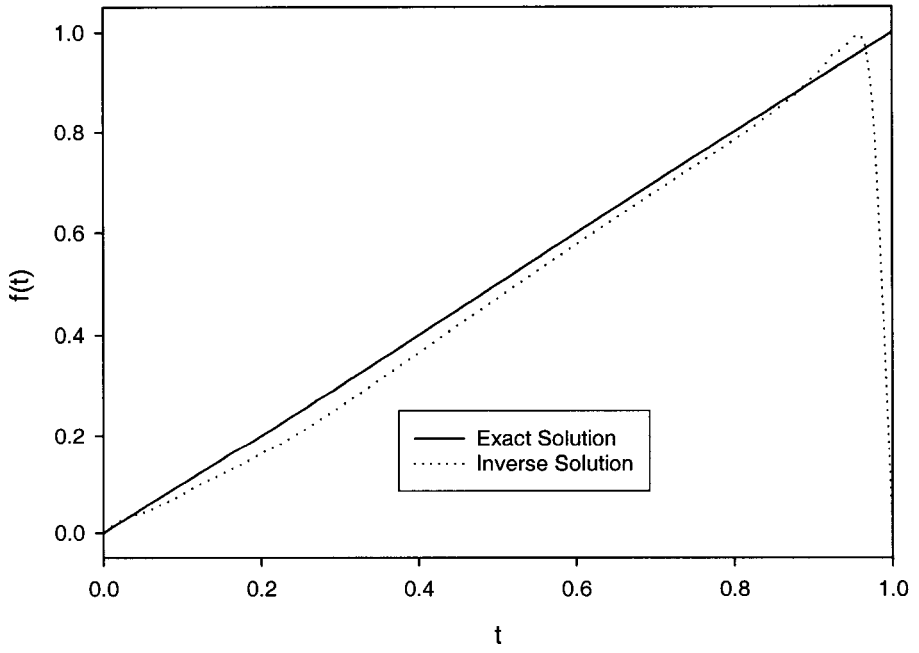

Figure 4.13 Concentration with Linear Profile at x = 0, Ra = 10^4, N=Le=ε=1

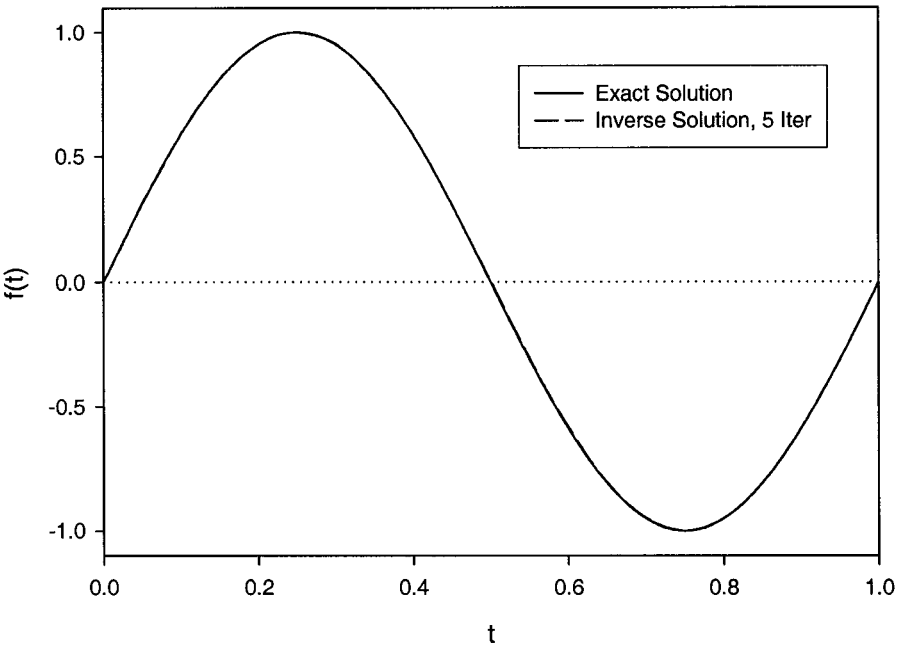

Figure 4.14 Inverse Solution for $f(t) = \sin(2\pi t)$ at $x = 0$, $Ra = 10^4$, $N=Le=\varepsilon=1$

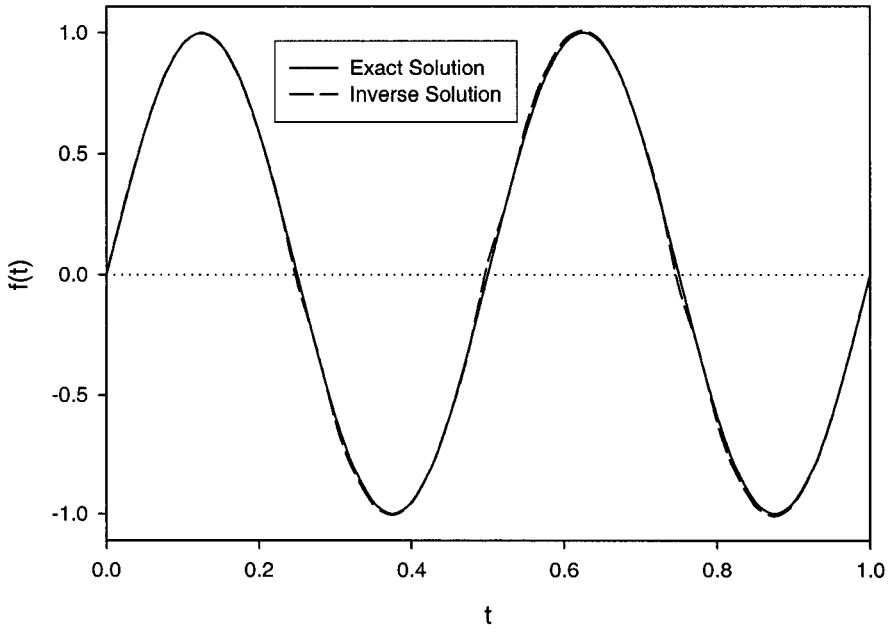

Figure 4.15 Inverse Solution for $f(t) = \sin(4\pi t)$ at $x = 0$, $Ra = 10^4$, $N=Le=\varepsilon=1$

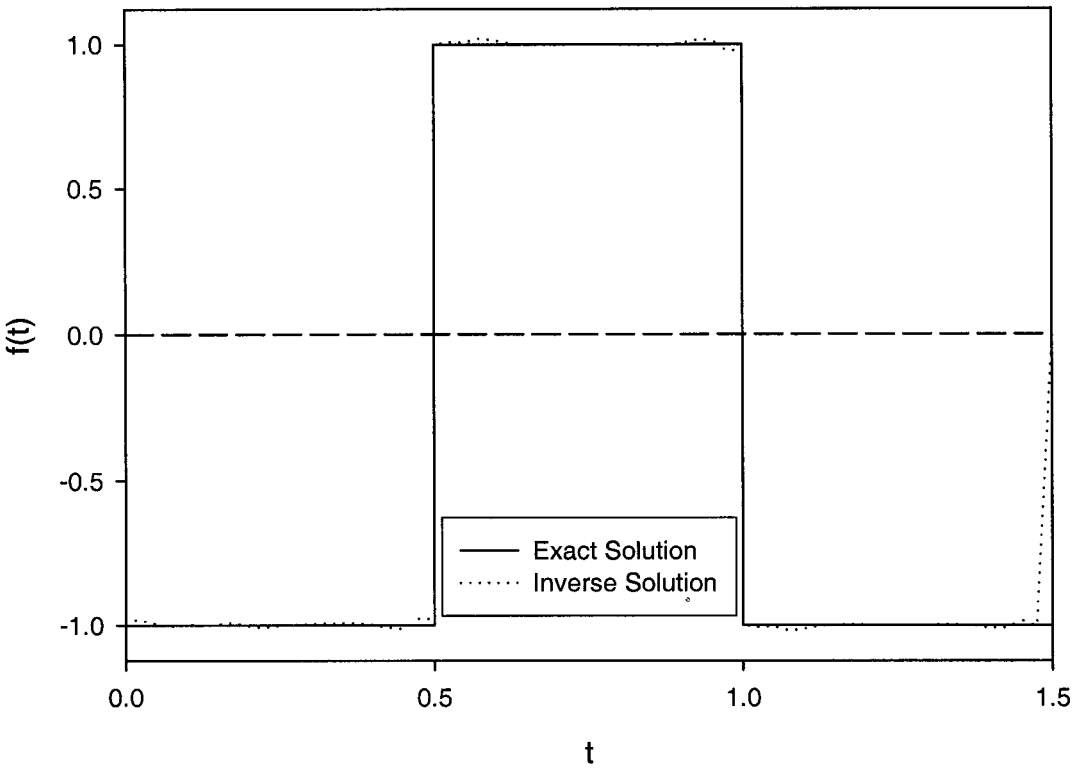

Figure 4.16 Concentration with Pulse Profile at x = 0, Ra = 10^4, N=Le=ε=1

❖ **Effect of Noisy Data**

In order to simulate the errors encountered in actual measurements, the noisy data form $S_m(1+\sigma\Sigma)$ is used instead of the exact value S_m, where $|\Sigma|<1$ is a uniformly distributed random real number. The influence of noisy input data on the inverse solution can be regularized using the discrepancy principle of Alifanov (the convergence criterion $\varepsilon = \sigma^2$) and CGM itself. Results for a noise of relative standard deviation σ = 0.02 and 0.05 are displayed in FIG.4.17 and FIG.4.18. The sine and triangular predicted profiles are reasonable accurate for σ at least up to 0.05. It is also an illustration of the applicability of the conjugate gradient method.

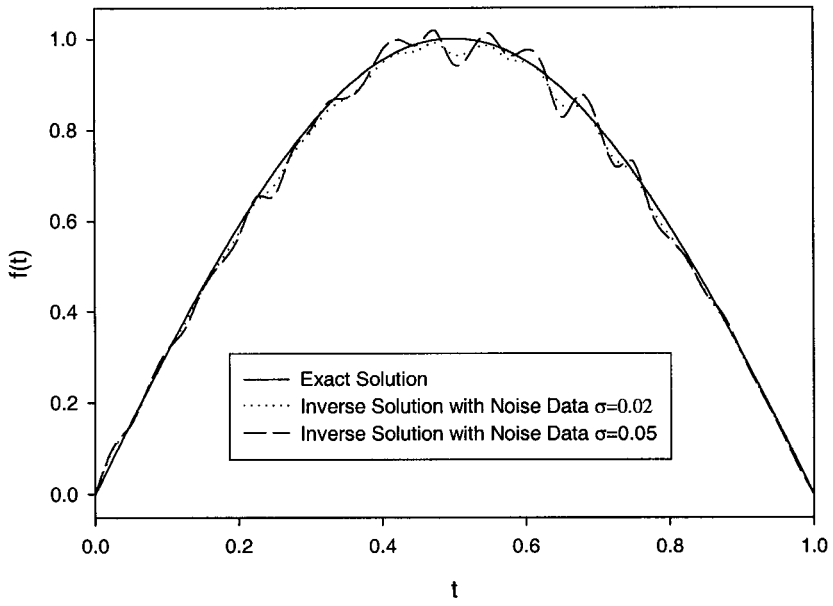

Figure 4.17 Inverse Solution for $f(t) = \sin(\pi t)$ with Noise Data, $Ra = 10^4$, N=Le=ε=1

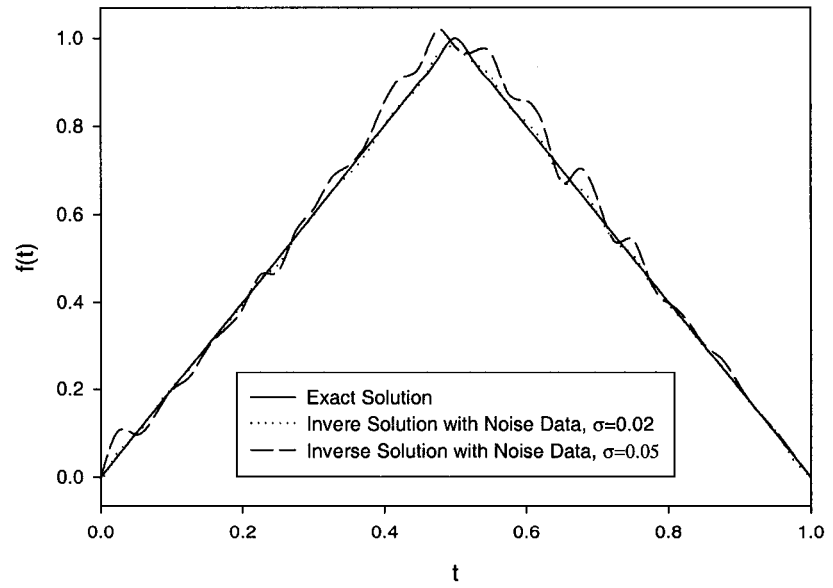

Figure 4.18 Inverse Solution for Triangular Concentration Profile with Noise Data

$Ra = 10^4$, N=Le=ε=1

❖ **Effect of Cavity Orientation**

To estimate the influence of the orientation of the cavity, we may rotate the system with an angle θ. If θ = π/2, the system will be heated from right wall, cooled from left wall; and the active boundary will be the bottom wall. FIG.4.19 suggests that the influence of the Rayleigh number on the solution accuracy is felt more rapidly as Ra increases than for θ = 0. When Ra=3000, the relative error of inverse solution is greater than 10% no matter how close to the active boundary the sensor are placed. So the range of Ra, Le and N for obtaining reasonably accurate inverse solution is different for different orientations which may change the whole concentration field.

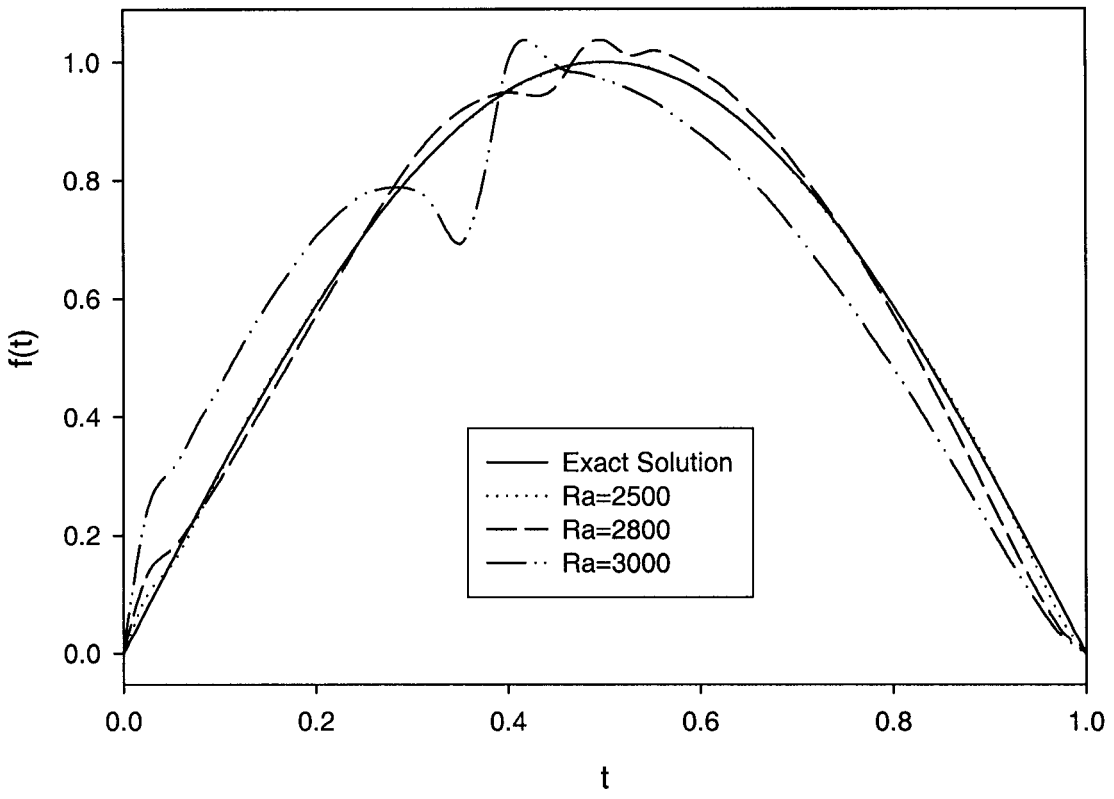

Figure 4.19 Inverse Solution for f(t) = sin(πt) at x = 0, N=Le=ε=1, $\theta = \frac{\pi}{2}$

4.2 Results for Non-uniform Concentration Profile on Active Boundary

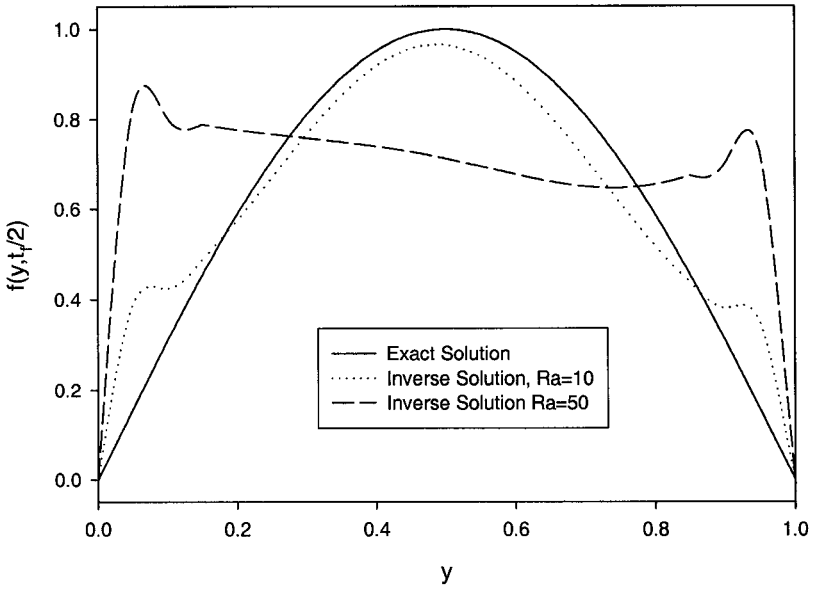

Figure 4.20a Inverse Solution for f(y, t) = sin(πt) sin(πy) at x = 0 t=t_f/2, N=Le=ε=1

Sensors at x=0.5L, $\theta = 0$

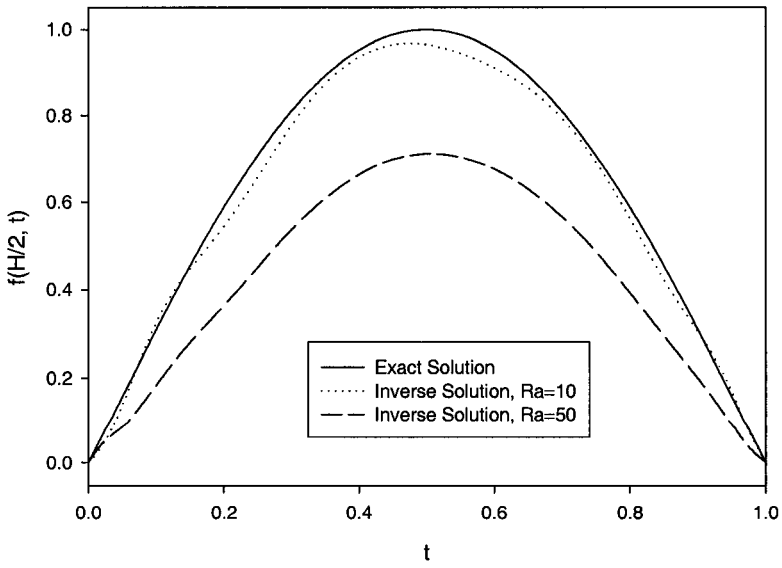

Figure 4.20b Inverse Solution for f(y, t) = sin(πt) sin(πy) at x = 0 y=H/2, N=Le=ε=1

Sensors at x=0.5L, $\theta = 0$

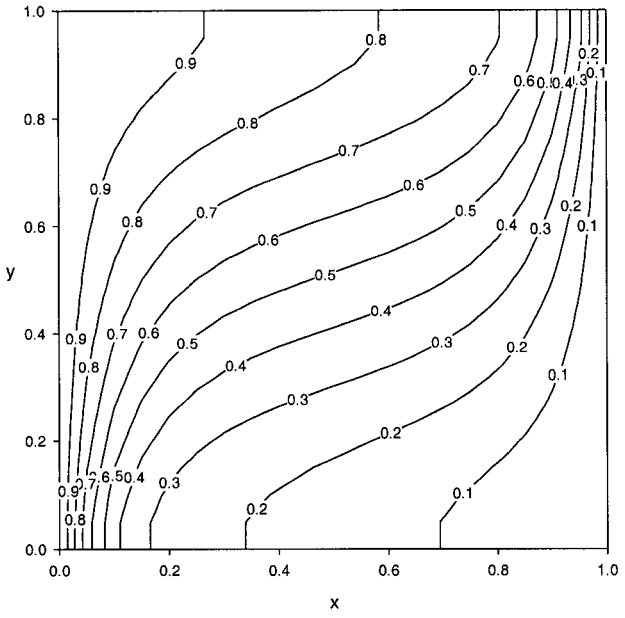

Figure 4.21a Solute concentration at $t_f/2$
Ra = 100, θ = 0, f(t) = sin(πt)

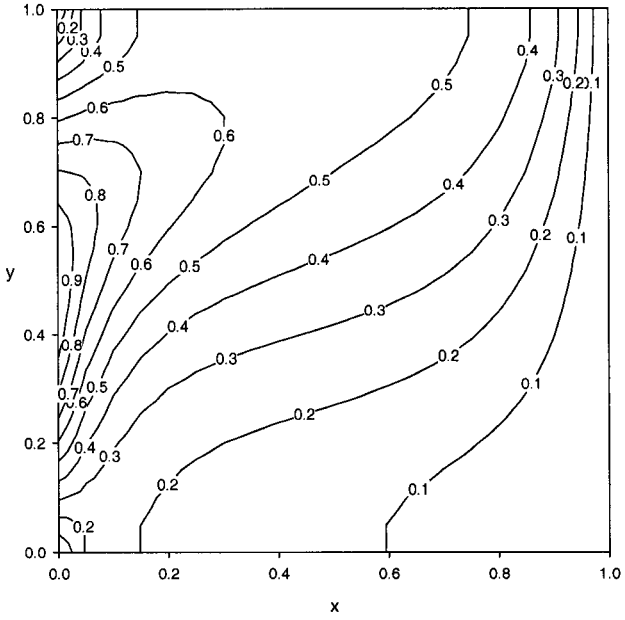

Figure 4.21b Solute concentration at $t_f/2$
Ra = 100, θ = 0, f(y,t) = sin(πy)sin(πt)

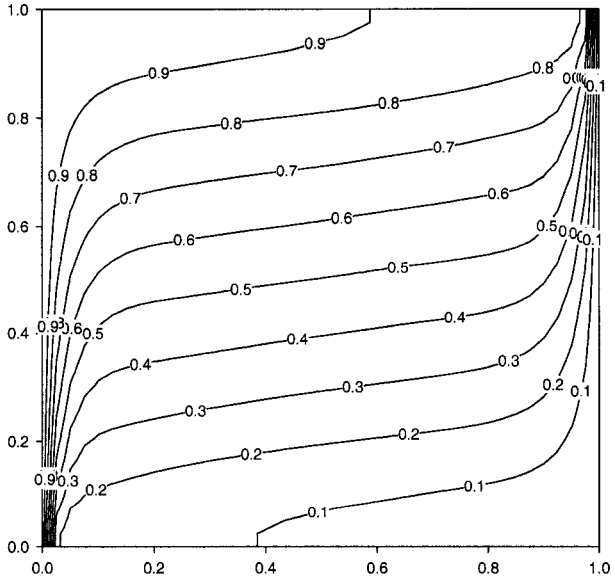

Figure 4.22a Solute concentration at $t_f/2$
Ra = 1000, θ = 0, f(t) = sin(πt)

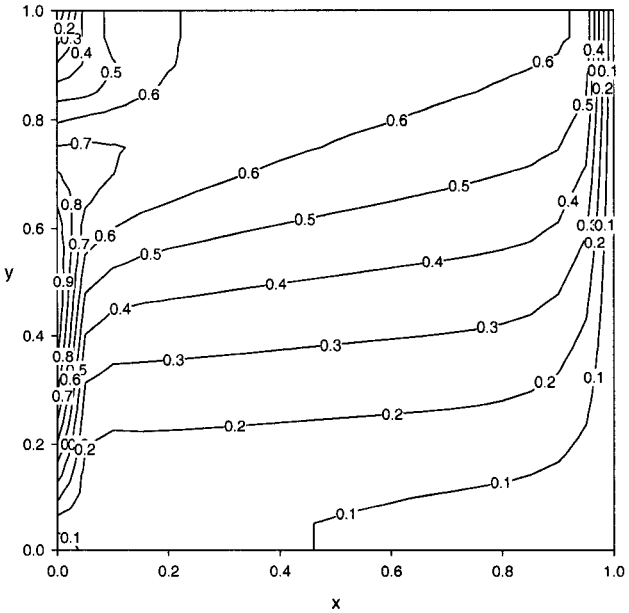

Figure 4.22b Solute concentration at $t_f/2$
Ra = 1000, θ = 0, f(y,t) = sin(πy)sin(πt)

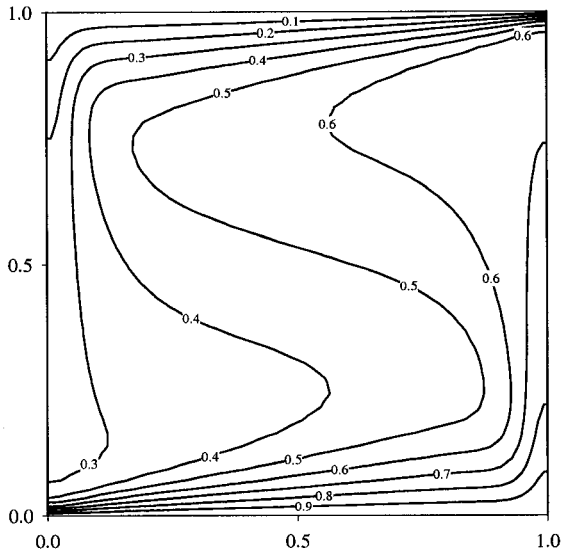

Figure 4.23a
Solute concentration at $t_f/2$, Ra = 1000
$f(t) = \sin(\pi t)$, $\theta = \pi/2$

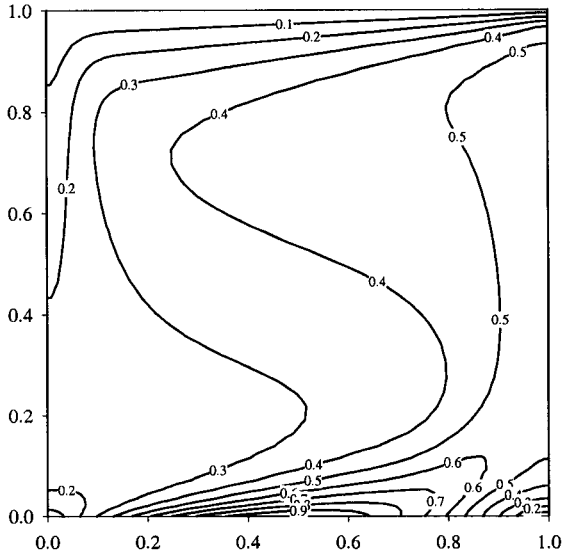

Figure 4.23b
Solute concentration at $t_f/2$, Ra = 1000
$f(y,t) = \sin(\pi y)\sin(\pi t)$, $\theta = \pi/2$,

The expected concentration on the active boundary is normally not-uniform in practice. The case f=f(y, t) should be considered. As we have discussed, one sensor is not enough. A series of sensors must be embedded at each calculation node on a line parallel to the active boundary. For the boundary conditions supposed in chapter I, however, the inverse solution is prone to be uniform along the direction of y (see FIG. 4.20a and FIG. 4.20a) even at low Rayleigh number if the sensors are located at x=0.5L. We may guess this phenomenon is physical and present independently of Rayleigh number, Lewis number and other parameters. Further study proved our supposition right. FIG.4.21, FIG.4.22 and FIG.4.23 show the comparison of concentration field between the case f=f(t) and the case f=f(y, t). We find that the boundary layer is intermittent and isoconcentration lines are not symmetric for the latter, which reveals a fairly complex behavior. But both isoline patterns in most of the area which is far from the boundary are very similar. In other words, the concentration in such region is not sensitive to the variation along y on active boundary. And then, the only way to improve the solution accuracy is by moving the sensors close to the active boundary.

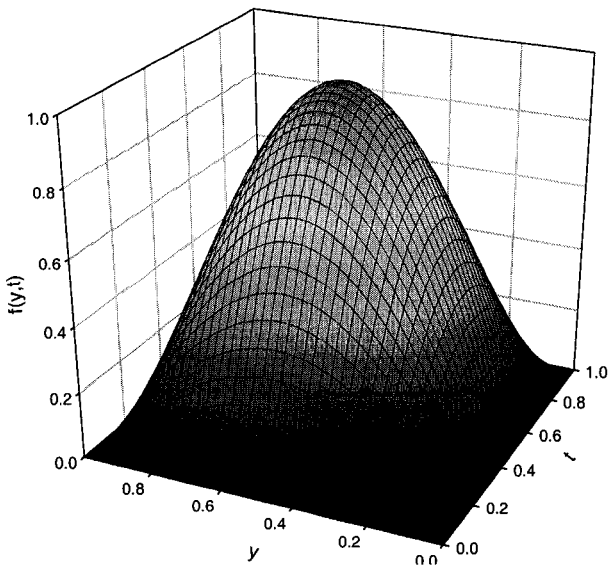

Figure 4.24a

Direct Solution at Ra = 1000
θ = 0, f(y, t) = sin(πy)sin(πt)

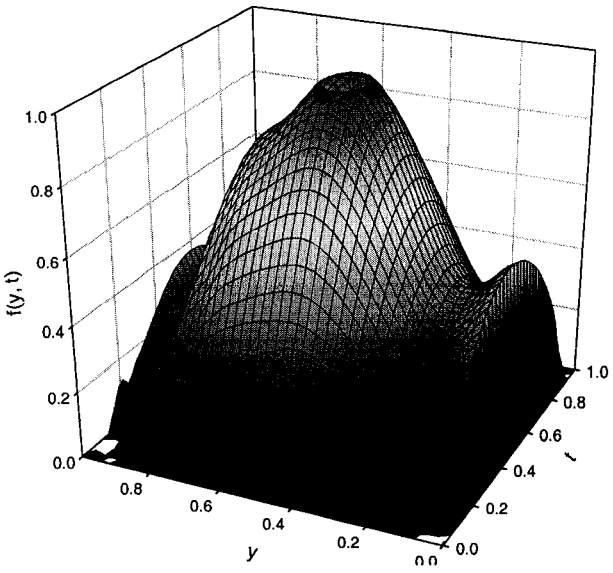

Figure 4.24b

Inverse Solution at Ra = 1000
θ = 0, f(y,t) = sin(πy)sin(πt), Sensors at x=0.1L

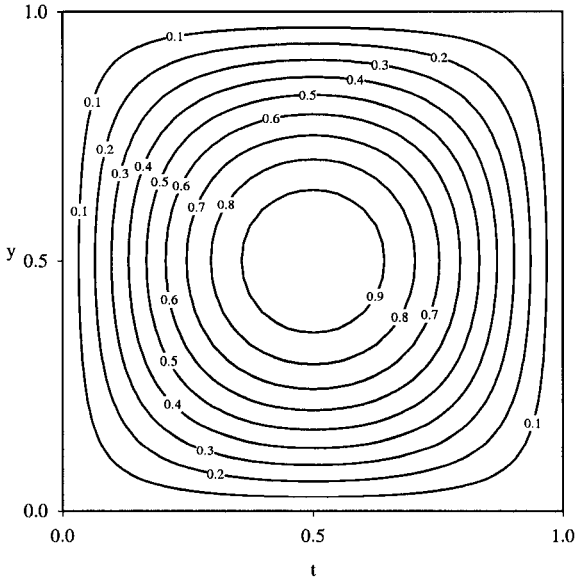

Figure 4.25a
Direct Solution at Ra = 1000
θ = π/2, f(y, t) = sin(πy)sin(πt)

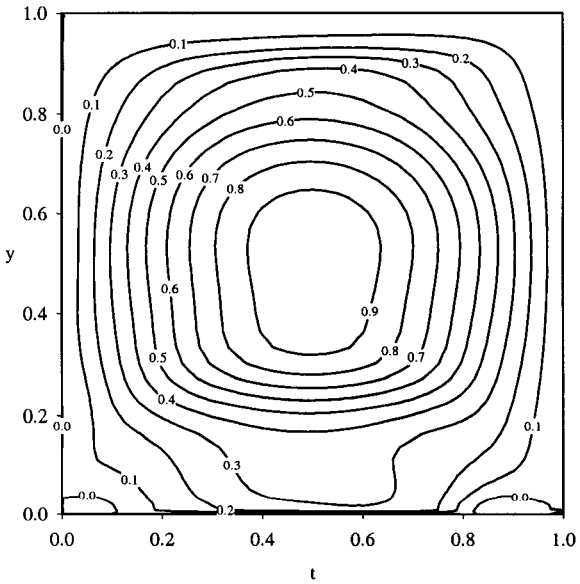

Figure 4.25b
Inverse Solution at Ra = 1000, θ = π/2
f(y, t) = sin(πy)sin(πt) , Sensors at x = 0.15L

If the sensors are placed at x=0.1L, acceptable numerical solutions for $\theta = 0$ can be obtained up to Ra = 1000, as shown in FIG.4.24. When Ra>1000, nothing can be done to prevent inverse solution divergence even if the sensors are put closer to the active boundary. Comparing FIG.4.22 with FIG.4.23, we find that the concentration field is more complex especially the boundary layer for $\theta = 0$. So for the case $\theta = \pi/2$, the solution accuracy should be better for present boundary conditions.

FIG.4.25 displays the comparison between the direct solution and inverse solution at Ra=1000, sensors are placed at x=0.15L and $\theta = \pi/2$. It clearly reveals that the variation along y of the concentration profile is much more difficult to reproduce than the variation with time. At Ra=2000 and 3000, we still get reasonable results for $\theta = \pi/2$ (see FIG.4.26 and FIG.4.27). If Ra>3000, the inverse solution may be divergent.

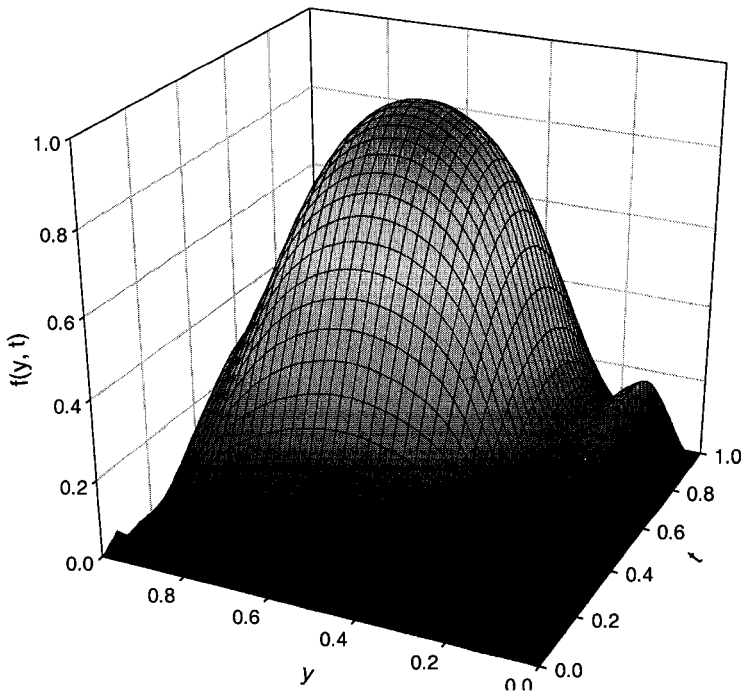

Figure 4.26 Inverse Solution at Ra = 2000, $f(y, t) = \sin(\pi y)\sin(\pi t)$
Sensors at x = 0.10L, $\theta = \pi/2$

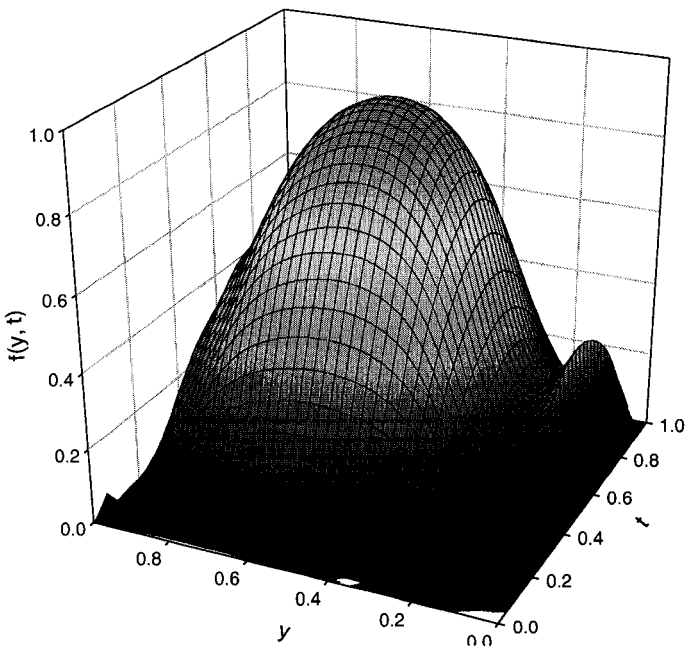

Figure 4.27a Inverse Solution at Ra = 3000, f(y, t) = sin(πy)sin(πt)
Sensors at x = 0.10L, θ = π/2, 3D View

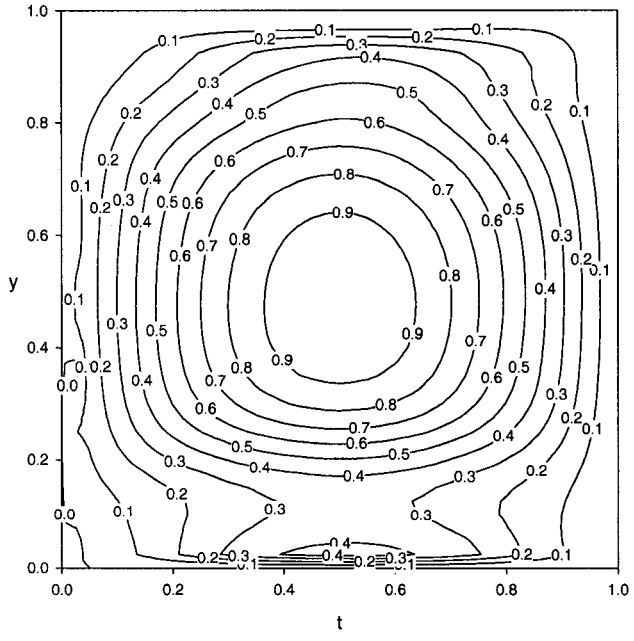

Figure 4.27b Inverse Solution at Ra = 3000, f(y, t) = sin(πy)sin(πt)
Sensors at x = 0.10L, θ = π/2, 2D View

CONCLUSION

The main objective of this study is to solve the inverse natural convection problem with double diffusion in a 2-D rectangular porous enclosure. Such an inverse problem can be transformed into an unconstrained optimization problem based on adjoint equation approach and regularized by iterative conjugate gradient method. The derivation of general sensitivity and adjoint equations is mathematically strict as introduced in Chapter II. All the partial differential equations are discretized by control volume method; the detail can be seen in Chapter III.

The time dependant formulation is tested for uniform as well as non-uniform concentration on active boundary. According to the results and subsequent discussion which was presented in Chapter IV, the following conclusions can be drawn:

1. The CG method is able to precisely predict uniform concentrations on the active boundary varying with time from concentration measured by a sensor within the porous enclosure ranging $0 < Ra \leq 10^4$, $0 < N \leq 10$ and $0 < Le \leq 5$.

2. The inverse solution is not very sensitive to the variation of ε ranging between 0.1 and 1.0. The coefficient ε is normally greater than 0.2 and less than 0.7 in engineering applications.

3. The CG method has good adaptability to various unknown concentration profiles. No matter the profile is linear, triangular, sinusoidal or other type, the reasonably accurate solutions can always be obtained.

4. The accuracy of the inverse solution is much influenced by boundary conditions that may decide the concentration field. For a cavity heated from the right boundary, cooled from the left wall, and concentration diffusing from bottom to top, more iterations and changing the sensor position cannot do any improvement to the final results when Ra>3000.

5. The sensors should be placed as close as possible to the active boundary. It brings more precise solutions or decreases the number of iteration, since the points rather near the active wall will make a quicker and more sensitive response to the variation of concentration on boundary.

6. Reasonable solutions may be obtained from noisy input data for σ at least up to 0.05. The regularization is done through stopping the iteration process according to the discrepancy principle of Alifanov before the high frequency components of the noise start to impair solution accuracy. It is also a proof that conjugate gradient method can be applied in real engineering practice.

7. For the case where concentration profile on active boundary is only time dependent, just one sensor within the system is enough. However, for the case where unknown concentration is time and space dependent, the concentration value at each node on a line parallel to the active boundary must be measured.

8. The inverse solutions for time dependant and non-uniform unknown concentration profiles are always prone to uniformity along the direction of y under the present boundary conditions even at low Rayleigh number. Moving the sensors rather close to the active boundary is the only way to improve the solution accuracy. The reasonable solution can be obtained for Rayleigh number up to an order of 10^3

depending on the precise form of the boundary conditions. The solution may be divergent and no procedure can improve the accuracy as Ra increases more. The results reveal that the regularization of conjugate gradient method is inefficient or low-efficient for the cases in which the boundary layer is intermittent.

REFERENCES

[1] KELLER, J.B. (1976), Inverse Problems, Amer. Math. Monthly 83, P107-118

[2] HEINZ, W.E., HANKE, M. and NEUBAUER, A. (1996), Regularization of Inverse Problems, Kluwer Academic Publishers

[3] ALIFANOV, O.M. (1994), Inverse Heat TransferProblems, Springer-Verlag, New York

[4] CHEN, J. (1998), Inverse Heat Conduction Problem in a Cavity, M.Sc.A. Thesis Mechanical Engineering, Ecole Polytechnique de Montreal

[5] HADAMARD, J. (1923), Lecture on Cauchy's Problem in Linear Partial Differential Equations, Yale University Press, New Haven, CT

[6] BECERRIL, R. and MENDOZA, J. (2001), Tricritical Behavior in Stationary Double Diffusive Convection with Cross Diffusion, Revista Mexicana de Fisica 48(2): 88-91

[7] MAMOU, M., VASSEUR, P. and BILGEN, E. (1998), A Galerkin Finite-Element Study of the Onset of Double-Diffusive Convection in an Inclined Porous Enclosure, Int. J. Heat Mass Transfer Vol.41 No.11, pp1513-1529

[8] STERN, M. (1960), The Salt Fountain and Thermohaline Convection, Tellus 12, 172

[9] STOMMEL, H., ARONS, A., and BLANCHARD, D. (1956), An Oceanographical Curiosity: The Perpetual Salt Fountain, Deep-Sea Res. 3, 152

[10] KELLY, D.E. (2001), Six Questions about Double Diffusive Convection

[11] KALLA, L. and VASSEUR, P. (2001), Double Diffusive Convection within a Horizontal Porous Layer Salted From the Bottom and Heated Horzontally

[12] PRUD'HOMME, M. and JASMIN, S. (2003), Int. J. Heat Mass Transfer, ??, pp. ?? (under press)

[13] LIN, R.T. (1995), Fundamental Heat and Mass Transfer in Porous Media

[14] BEAR, J. (1972), Dynamics of Fluids in Porous Media, American elsevier publishing company, Inc, New York

[15] BEAR, J. and BECHMAT, Y. (1991), Introduction to Modeling of Transport Pheonomena in Porous Media, Kluwer Academic Publishers

[16] SLATTERY, J.C. (1972), Momentum, Energy and Mass Transfer in Continua, Mc-Graw Hill, New York

[17] TAYLOR, J. and ZIMA, W. (1999), Solution of Inverse Heat Conduction Problems Using Control Volume Approach, Int. J. Heat Mass Transfer, 42, 1123-1140

[18] YANG, C.Y. (1998), Solving the Two-Dimensional Inverse Heat Source Problem Through the Linear Least-Squares Error Method, Int. J. Heat Mass Transfer 41 (2), 393-398

[19] TARANTOLA, A. and VALETTE, B. (1982), Generalized Nonlinear Inverse Problems Solved Using the Least-Squares Criterion, Reviews of Geophysics and Space Physics, Vol. 20, No. 2, pp 219-232

[20] TIKHONOV, A.N. (1977), Solution of Ill-Posed Problems, Halsterd Press

[21] RAMOS, F. and GIOVANNINI, A. (1995), Resolution of Multimentional Heat Diffusive Inverse Problem by Analytical Elements Method and Principle of Maximum Entropy, Int. J. Heat and Mass Transfer 38 (1), 101-111

[22] HANSEN, P.C. (1994), Regularization Tools for Analysis and Solution of Discrete Ill-Posed Problems, Numerical Algorithms, 6, pp.1-35

[23] BECK, J.V., BLACKWELL and CLAIR, S. (1985), Inverse Heat Conduction: Ill-posed Problems

[24] DIEGO, M. (1993), The Mollification Method and the Numerical Solution of Ill-Posed Problems, John Wiley and Sons

[25] PRUD"HOMME, M. and NGUYEN, T.H. (2000), Solution of Inverse Free Convection Problems by Conjugate Gradient Method: Effects of Rayleigh Number, International Journal of Heat and Mass Transfer

[26] PRUD"HOMME, M. and NGUYEN, T.H. (1999), Fourier Analysis of Conjugate Gradient Method Applied to Inverse Heat Conduction Problems, International Journal of Heat and Mass Transfer

[27] TARANTOLA, A. (1987), Inverse Problem Theory, Elsevier

[28] MOSEGAARD, K. and TARANTOLA, A. (2002), Probabilistic Approach to Inverse Problems, Academic Press, page 237-265

[29] BECK, J.V. (1970), Nonlinear Estimation Applied to the Nonlinear Inverse Heat Conduction Problems, Int. J. Heat Mass Transfer, 13, pp. 703-716

[30] MOUTSOGLOU, A. (1989), An Inverse Convection Problem, ASME J. Heat Transfer, 221, pp. 37-43

[31] PARK, H.M. and CHUNG, O.Y. (1999), An Inverse Natural Convection Problem of Estimating the Strength of a Heat Source, Int. J. Heat Mass Transfer, 42, pp. 4259-4273

[32] PARK, H.M and JUNG, W.S. (2000), The Karhunen-Loeve Galerkin Method For the Inverse Natural Convection Problem, Int. J. Heat Mass Transfer

[33] PRUD'HOMME, M. and NGUYEN, T.H. (2000), Solution of Inverse Free Convection Problems By Conjugate Gradient Method: Effects of Rayleigh Number, Int. J. Heat Mass Transfer

[34] ZABARAS, N. and YANG, G. (1997), A Functional Optimization Formulation and Implementation of An Inverse Natural Convection Problem, Comp. Meth. in Appl. Mec. and Eng., 144, No.3, pp. 245-274

[35] ZHANG, X.L. (1989), Wave Number Selection in Penetrative Convection, Ph.D. Thesis Mechanical Engineering, Ecole Polytechnique de Montreal

[36] BEJAN, A. (1984), Convection Heat Transfer, A Wiley-Intersscience Publication, New York

[37] GUO, K.L., KONG, X.Q. and CHEN, S.N. (1988), Computational Heat Transfer, China Science and Technology University Press, Hefei

[38] FLETCHER, R. (1987), Practical Methods of Optimization, John Wiley & Sons

[39] COOPER and STEINBERG (1970), Introduction to Methods of Optimization, W.B. Saunders Company

[40] XI, S. L. and ZHAO, F. Z. (1989), Optimized Methods

[41] PATANKAR, S.V. (1980), Numerical Heat Transfer and Fluid Flow, Hemisphere Publishing Corporation

[42] PRUD'HOMME, M. and JIANG, H. (2003), Inverse Determination of Concentration In Porous Medium With Thermosolutal Convection, Int. C. Heat Mass Transfer, 30, pp. 303-312